

AD _____

GRANT NUMBER: DAMD17-96-1-6250

TITLE: IGF-IR SIGNALING IN BREAST CANCER

PRINCIPAL INVESTIGATOR: EWA SURMACZ, PH.D.

RECIPIENT ORGANIZATION: THOMAS JEFFERSON UNIVERSITY
KIMMEL CANCER INSTITUTE
PHILADELPHIA, PA 19107

REPORT DATE: September 1997

TYPE OF REPORT: ANNUAL

PREPARED FOR: Commander
U.S. Army Medical Research and Materiel Command
Fort Detrick, Frederick, Maryland 21702-5012

DISTRIBUTION STATEMENT: Approved for public release;
distribution unlimited

The views, opinion and/or findings contained in this report are those of the author(s) and should not be construed as an official Department of the Army position, policy or decision unless so designated by other documentation.

DTIC QUALITY INSPECTED 2

19971001 016

REPORT DOCUMENTATION PAGE

Form Approved

OMB No. 0704-0188

Public reporting burden for this collection of information is estimated to average 1 hour per response, including the time for reviewing instructions, searching existing data sources, gathering and maintaining the data needed, and completing and reviewing the collection of information. Send comments regarding this burden estimate or any other aspect of this collection of information, including suggestions for reducing this burden, to Washington Headquarters Services, Directorate for Information Operations and Reports, 1215 Jefferson Davis Highway, Suite 1204, Arlington, VA 22202-4302, and to the Office of Management and Budget, Paperwork Reduction Project (0704-0188), Washington, DC 20503.

1. AGENCY USE ONLY (Leave blank)		2. REPORT DATE September 1997	3. REPORT TYPE AND DATES COVERED Annual (15 Aug 96 - 14 Aug 97)	
4. TITLE AND SUBTITLE IGF-IR SIGNALING IN BREAST CANCER			5. FUNDING NUMBERS DAMD17-96-1-6250	
6. AUTHOR(S) EWA SURMACZ, PH.D.				
7. PERFORMING ORGANIZATION NAME(S) AND ADDRESS(ES) THOMAS JEFFERSON UNIVERSITY KIMMEL CANCER INSTITUTE PHILADELPHIA, PA 19107			8. PERFORMING ORGANIZATION REPORT NUMBER	
9. SPONSORING/MONITORING AGENCY NAME(S) AND ADDRESS(ES) COMMANDER U.S. ARMY MEDICAL RESEARCH AND MATERIEL COMMAND FORT DETRICK, FREDERICK, MARYLAND 21702-5012			10. SPONSORING/MONITORING AGENCY REPORT NUMBER	
11. SUPPLEMENTARY NOTES				
12a. DISTRIBUTION / AVAILABILITY STATEMENT APPROVED FOR PUBLIC RELEASE; DISTRIBUTION UNLIMITED			12b. DISTRIBUTION CODE	
13. ABSTRACT (Maximum 200) Experimental and clinical evidence suggests that the insulin-like growth factor (IGF) system is involved in the growth of breast cancer cells in vitro and may be important in breast cancer etiology and progression. The IGF-IR is overexpressed in breast cancer cells compared with its levels in normal breast epithelium, and high levels of IGF-IR, or its major substrate IRS-1, correlate with tumor recurrence. Paradoxically, high levels of IGF-IR are associated with better prognosis. Thus, the mechanisms by which abnormal activation of the IGF-IR regulates breast tumor development and progression are not clear. We have developed an in vitro model to investigate the role of the IGF-IR and its different signaling pathways in the emergence of such tumor characteristics as estrogen independence, enhanced autonomous growth, altered motility and cell-cell connections, all of which are determinants of tumor progression. Using cell lines expressing different levels of the IGF-IR, or cells with down-regulated expression of IGF-IR signaling molecules, we demonstrated that overexpressed IGF-IRs promote cell survival in three-dimensional culture by enhancing E-cadherin mediated intercellular adhesion. The IRS-1 signaling pathway is critical for cell survival and resistance to antiestrogens.				
14. SUBJECT TERMS BREAST CANCER			15. NUMBER OF PAGES 47	
			16. PRICE CODE	
17. SECURITY CLASSIFICATION OF REPORT UNCLASSIFIED	18. SECURITY CLASSIFICATION OF THIS PAGE UNCLASSIFIED	19. SECURITY CLASSIFICATION OF ABSTRACT UNCLASSIFIED	20. LIMITATION OF ABSTRACT UNLIMITED	

FOREWORD

Opinions, interpretations, conclusions and recommendations are those of the author and are not necessarily endorsed by the U.S. Army.

____ Where copyrighted material is quoted, permission has been obtained to use such material.

____ Where material from documents designated for limited distribution is quoted, permission has been obtained to use the material.

AS Citations of commercial organizations and trade names in this report do not constitute an official Department of Army endorsement or approval of the products or services of these organizations.


____ In conducting research using animals, the investigator(s) adhered to the "Guide for the Care and Use of Laboratory Animals," prepared by the Committee on Care and Use of Laboratory Animals of the Institute of Laboratory Resources, National Research Council (NIH Publication No. 86-23, Revised 1985).

____ For the protection of human subjects, the investigator(s) adhered to policies of applicable Federal Law 45 CFR 46.

AS In conducting research utilizing recombinant DNA technology, the investigator(s) adhered to current guidelines promulgated by the National Institutes of Health.

AS In the conduct of research utilizing recombinant DNA, the investigator(s) adhered to the NIH Guidelines for Research Involving Recombinant DNA Molecules.

AS In the conduct of research involving hazardous organisms, the investigator(s) adhered to the CDC-NIH Guide for Biosafety in Microbiological and Biomedical Laboratories.

 July 15, 1997

PI - Signature Date

TABLE OF CONTENTS

	Pg.
Report Documentation Page	2
Foreword	3
Table of Contents	4
Introduction	5
Technical Report	6
Conclusions	8
References	9
Appendix	11

INTRODUCTION

There is experimental evidence that the insulin-like growth factor (IGF) system (IGF-I, IGF-II, IGF-I receptor [IGF-IR], and IGF-I binding proteins [IGFBP]) is involved in the growth of breast cancer cells in vitro (1-6). Clinical data, although scarce, also suggest a role of the IGF system in breast cancer etiology (1,2,7-9). For instance, the IGF-IR is overexpressed in breast cancer cells compared with its levels in normal breast epithelium (7); insulin receptor substrate 1 (IRS-1), a major substrate of the IGF-IR, is overexpressed in tumors with shorter disease-free survival (9); high levels of IGF-IR correlate with primary tumor recurrence following lumpectomy and radiotherapy (8); certain IGFBP are downregulated in breast tumors possibly allowing greater IGF bioavailability (1). Interestingly however, high levels of IGF-IR are associated with better prognosis and a more differentiated tumor phenotype (7).

Thus, the mechanisms by which abnormal activation of the IGF-IR may contribute to the development and progression of breast tumors are not clear. One important consequence of the amplification of IGF-IR signaling might be the development of estrogen-independence. Often, the growth of breast cancer cells is under synergistic control of polypeptide growth factors such as IGFs and steroid hormones such as estrogen (1). Overexpression of growth factor receptors or signaling molecules may result in loss of steroid requirements and estrogen-independence. This may lead to the development of anti-estrogen resistance. Amplification of IGF-IR signaling may facilitate tumor progression by endowing the cells with enhanced survival abilities (4).

Studying IGF-IR-related alterations in breast cancer phenotype requires a well characterized cellular model. Consequently, the goal of this project was developing such a model consisting of a collection of breast cancer cell lines expressing different levels of either the IGF-IR or its signaling intermediates. With these cells we planned to investigate the role of the IGF-IR and its different signaling pathways in the development of such tumor characteristics as estrogen independence, enhanced mitogenicity and transforming potential, enhanced motility, and altered cell-cell connections (all of which are determinants of tumor progression). In addition, we intended to correlate the alterations in the phenotype of breast cancer cells with the levels of the overexpressed molecules.

The following specific aims have been proposed:

1) To test the effects of the amplification of IGF-IR signaling on the growth and transformation of estrogen-sensitive breast cancer cells.

To this end, the wild-type IGF-IR will be overexpressed in MCF-7 human breast cancer cells, and several clones expressing different levels will be developed. The new phenotype of the cells will be determined by studies of monolayer and anchorage-independent growth, cell motility, and cell-cell adhesion. Estrogen-dependence of the cells will be determined under the above studied conditions.

2) To determine which domains of the IGF-IR and which elements of the IGF-IR signaling are required to establish a more neoplastic phenotype in MCF-7 cell.

3) To test the ability of various molecular strategies targeted at the IGF-IR signaling to reverse the neoplastic phenotype of breast cancer cells.

In aims 2 and 3, different IGF-IR mutants will be overexpressed in MCF-7 cells, and the ability of these mutant receptors to alter the neoplastic phenotype of breast cancer cells will be determined. Similarly, the phenotype of MCF-7 cells overexpressing different signaling molecules such as IRS-1, SHC, or GRB2 will be analyzed. The importance of these signaling elements in the maintenance of the neoplastic phenotype of breast cancer cells will be evaluated by antisense RNA strategy.

4) To study the immediate effects of estradiol stimulation on the activation of the IGF-IR signaling pathway in breast cancer cells.

The acute effects of estradiol on tyrosine phosphorylation of the IGF-IR, IRS-1, and SHC, as well as on the activation of further downstream signaling pathways will be examined.

TECHNICAL REPORT

The experiments proceeded according to the Statement of Work.

We investigated whether amplification of IGF signaling in hormone-dependent breast cancer cells MCF-7 induces estrogen-independence and contributes to the development of a more neoplastic phenotype. To this end we generated, by stable transfection, several cell lines overexpressing the wild-type IGF-IR. By screening the clones using FACS analysis, Western blotting, and Scatchard assay, we developed a collection of clones overexpressing from 8 to 50-fold IGF-IR relative to the level in the parental cells (4).

The elevated level of the IGF-IR considerably enhanced responsiveness of cells to low doses of IGF (0.1 ng/ml) in the presence of estradiol (10 nM) in monolayer culture. With higher doses of IGF-I (4 ng/ml), the cells that overexpressed IGF-IRs exhibited estrogen-independence. Surprisingly, IGF-IR amplification did not provide growth advantage under anchorage-independent conditions (in soft agar), nor did it induce invasiveness or motility tested in modified Boyden chambers (4).

The consequences of IGF-IR overexpression appeared much more pronounced in cells cultured in three-dimensional culture (reminiscent of primary tumor growth) on the extracellular matrix (Matrigel) (4). In particular, high levels of IGF-IRs (over 1×10^6 receptors/cell) promoted aggregation of cells into large spheroids that were characterized by enhanced proliferation and prolonged survival compared with spheroids formed by the parental cells. Lower receptor levels (less than 1×10^6 sites/cell) supported formation of only small clusters and

did not protect from cell death. In all tested cell lines, aggregation was stimulated by IGF-I treatment. By indirect immunofluorescence, we found that the IGF-IR was localized at the points of cell-cell contacts. In MCF-7 cells and in the IGF-IR overexpressing clones, immunoprecipitation and Western blotting with specific antibodies provided evidence that E-cadherin, the major epithelial cell-cell adhesion molecule, was complexed with the IGF-IR and its two cellular substrates, IRS-1 and SHC. The mechanism by which IGF-IR regulates E-cadherin-mediated cell-cell adhesion is not known. Our preliminary results demonstrated that the stimulation of cells with IGF correlated with the decreased tyrosine phosphorylation of a 120 kDa protein, (possibly E-cadherin) in the adhesion complex (4).

[These data have been published in Experimental Cell Research (4)].

Our other goal was to establish the role of two major IGF-IR substrates, IRS-1 and SHC, in the maintenance of the phenotype of MCF-7 breast cancer cells. We approached this problem by creating MCF-7-derived cell lines in which the levels of either IRS-1 or SHC were down-regulated by the expression of antisense RNA (2). Two cell lines in which the levels of IRS-1 were decreased by ~80%, and two cell lines with ~ 50% downregulation of SHC levels were selected for further experiments. The cells were analyzed in monolayer and three-dimensional culture as well as in soft agar and in modified Boyden chambers. The results provided evidence that the IRS-1 pathway is critical for cell growth and for the protection from apoptosis, while the SHC pathway plays, appears to play a role in cell proliferation and is critical in the regulation of cell motility. Both pathways are involved in anchorage-independent growth. [These data have been accepted for publication in International Journal of Cancer (2)].

Our third aim was to study whether antiestrogens such as Tamoxifen were able to inhibit the growth of breast cancer cells with amplified IGF-IR signaling. In these studies, we used MCF-7 cells overexpressing 9-fold IRS-1 and MCF-7 cells with 20 and 50-fold IGF-IR overexpression. The cells were treated with different concentrations of Tamoxifen (0.1-100 nM) for 4 days. A 10nM dose of Tamoxifen was sufficient to inhibit by at least 50% the growth of all studied cell lines, regardless of the amplification of IGF-IR signaling. Thus, overexpression of IRS-1 or the IGF-IR did not induce an ER-negative phenotype and was not sufficient to circumvent the sensitivity of cells to the cytostatic effect of Tamoxifen in monolayer culture. Tamoxifen inhibited the autocrine and IGF-I-dependent growth of all tested cell lines, interfering with IGF-IR signaling. Specifically, a long-term treatment with tamoxifen (4 days) was accompanied by a continuous dephosphorylation of IRS-1 on tyrosine residues and abrogation of the IRS-1/PI-3 kinase signaling pathway. Interestingly, the SHC pathway appeared to be enhanced in growth arrested cells. [Published in Cancer Research (10)].

We have also studied acute effects of estrogen on IGF-IR signaling in MCF-7 cells. Several experiments in MCF-7 cells and MCF-7 cells overexpressing IRS-1 or the IGF-IR, demonstrated increased tyrosine phosphorylation of IRS-1 and SHC in response to 1 or 5 min estrogen treatment. Other experiments did not confirm these effects. Specifically, no immediate changes in the tyrosine phosphorylation status of the studied signaling molecules were noted in

estrogen treated cells. We are in the process of evaluating possible causes of this discrepancy. Preliminary data suggest that acute responses to hormone treatment are transient and may be dependent on cell culture density. In very confluent cells, for instance, acute response is not detected after 1 or 5 min treatment.

CONCLUSIONS

This project has been designed to understand whether the neoplastic progression of breast cancer cells may be regulated by abnormal activation of the IGF-IR signaling pathway. In particular, we investigated if enhanced IGF signaling would affect proliferation, hormone-dependence, tumorigenicity, survival in three-dimensional culture, and invasiveness of breast cancer cells, the features that are often associated with the development and progression of breast tumors. Our studies determined that increased levels of either IGF-IR or its substrate IRS-1 reduced estrogen requirements for growth, in consequence allowing the cells to proliferate in IGF alone. In addition, overexpression of the IGF-IR stimulated aggregation and survival of cells in three-dimensional culture. The results indicate that amplification of IGF signaling endows breast cancer cells with growth and survival advantage. This features may contribute to the development of tumor mass, and possibly, to facilitate the survival of tumor cells found in the circulation.

Our finding that the IGF-IR regulates intercellular adhesion and survival in three-dimensional culture is a novel one. Our laboratory provided the first evidence for a physical association between IGF-IR and a cell adhesion molecule, E-cadherin. We are also the first to indicate a critical role of IRS-1 signaling in two important processes: 1) survival of breast cancer cells, and 2) sensitivity to antiestrogens.

These results should help understanding the role of the IGF-IR in breast cancer etiology and progression. Moreover, by determining signaling pathways critical for cancer survival or spread, we will be able to design new targets for anti-growth factor therapy in breast cancer.

In the next budget period, we will 1) continue the studies on the mechanism of IGF-IR-dependent intercellular adhesion; 2) continue the work on antiestrogen interaction with IGF-IR signaling using pure antiestrogen ICI 182,780; 3) study the mechanism of SHC-dependent cell motility in breast cancer cells.

PUBLICATIONS and COMMUNICATIONS RESULTING FROM THIS WORK

Publications

1. Guvakova, M., and Surmacz, E. Overexpressed IGF-I receptors reduce estrogen growth requirements, enhance survival and promote E-cadherin-

mediated cell-cell adhesion in human breast cancer cells. *Exp. Cell Res.* 231: 149-162, 1997

2. Nolan, M., Jankowska, L., Prisco, M., Xu, S., Guvakova, M., and Surmacz, E. Differential roles of IRS-1 and SHC signaling pathways in breast cancer cell. *Int. J. Cancer*, in press

3. Guvakova, M., and Surmacz, E. Tamoxifen interferes with the insulin-like growth factor I receptor (IGF-IR) signaling pathway in breast cancer cells. *Cancer Research*, 57: 2606-2610, 1997

Scientific Communications and Talks

1. Guvakova, M., Surmacz, E. Overexpression of the IGF-IR, but not of its substrate IRS-1, stimulates E-cadherin-mediated cell-cell adhesion in human breast cancer cells. 49th Annual Symposium on Fundamental Cancer Research "Regulatory mechanisms in growth and differentiation", Houston, TX, October 22-25, 1996.

2. Surmacz, E. Mitogenic and transforming signaling of the IGF-IR. Department of Endocrinology, University of Catania, Italy, May 5, 1997 (invited speaker).

3. Surmacz, E. IGF-IR in breast cancer. Department of Pathology, University of Catania, Italy, May 6, 1997 (invited speaker).

4. Guvakova, M., Surmacz, E. Tamoxifen differentially modulates IGF-IR signaling pathways in breast cancer cells. The Endocrine Society 79th Annual Meeting, Minneapolis, June 11-14, 1997

5. Ando, S., Salerno, M., Sisci, D., Panno, M. L., Nolan, M. K., Surmacz, E. IRS-1 signaling and insulin-induced modulation of estrogen receptors in breast cancer. The Endocrine Society 79th Annual Meeting, Minneapolis, June 11-14, 1997

REFERENCES

1. Lee, A. V., Yee, D. Insulin-like growth factors and breast cancer. *Biomed. Pharmacother.* 49: 415-421, 1995.

2. Ellis, M.J.C., Singer, C., Hornby, A., Rasmussen, A., Cullen, K.J. Insulin-like growth factor mediated stromal-epithelial interactions in human breast cancer. *Breast Cancer Res. and Treat.*, 31: 249-261.1994.

3. Dunn, S.E., Hardman, R.A., Kari, F.W., Barrett, J.C. Insulin-like growth factor 1 (IGF-1) alters drug sensitivity of HBL100 human breast cancer cells by inhibition of apoptosis induced by diverse anticancer drugs. *Cancer Res.*, 57: 2687-2693, 1997.

4. Guvakova, M. A., Surmacz, E. Overexpressed IGF-I receptors reduce estrogen growth requirements, enhance survival and promote cell-cell adhesion in human breast cancer cells. *Exp. Cell Res.* 231: 149-162, 1997.
5. Surmacz, E., Burgaud, J-L. Overexpression of insulin receptor substrate 1 (IRS-1) in the human breast cancer cell line MCF-7 induces loss of estrogen requirements for growth and transformation. *Clin. Cancer Res.* 1: 1429-1436, 1995.
6. Cullen, K. J., Yee, D., Sly, W.S., Perdue, J., Hampton, B., Lippman, M.E., Rosen, N. Insulin-like growth factor receptor expression and function in human breast cancer. *Cancer Res.*, 50: 48-53, 1990.
7. Pezzino, V. , Papa, V., Milazzo, G., Gliozzo, B., Russo, P., Scalia, P. L. Insulin-like growth factor-I (IGF-I) receptors in breast cancer. *Ann NY Acad Sci* 784: 189-201, 1996.
8. Turner, B.C., Haffty, B.G., Narayanann, L., Yuan, J., Havre, P.A., Gumbs, A., Kaplan, L., Burgaud, J-L., Carter, D/, Baserga, R., Glazer, P.M. IGF-I receptor and cyclin D1 expression influence cellular radiosensitivity and local breast cancer recurrence after lumpectomy and radiation. *Cancer Res.*, 1997, in press
9. Rocha, R. L., Hilsenbeck, S. G., Jackson, J. G., Van Der Berg, C. L., Weng, C-W., Lee, A. V. Yee, D. Insulin-like growth factor binding protein 3 and insulin receptor substrate 1 in breast cancer: correlation with clinical parameters and disease-free survival. *Clin. Cancer Res.* 3: 103-109, 1997.
10. Guvakova, M. A., Surmacz, E. Tamoxifen interferes with the insulin-like growth factor I receptor (IGF-IR) signaling pathway in breast cancer cells. *Cancer Res.* 57: 2606-2610, 1997.

APPENDIX

Manuscripts:

1. Guvakova, M., Surmacz, E. Overexpressed IGF-I receptors reduce estrogen growth requirements, enhance survival and promote cell-cell adhesion in human breast cancer cells. (pg. 12-25)
2. Guvakova, M., Surmacz, E. Tamoxifen interferes with the insulin-like growth factor I receptor (IGF-IR) signaling pathway in breast cancer cells. (pg. 26-30)
3. Nolan, M., Jankowska, L., Prisco, M., Xu, S., Guvakova, M., Surmacz, E. Differential roles of IRS-1 and SHC signaling pathways in breast cancer cells. (pg. 31-47)

Overexpressed IGF-I Receptors Reduce Estrogen Growth Requirements, Enhance Survival, and Promote E-Cadherin-Mediated Cell–Cell Adhesion in Human Breast Cancer Cells

MARINA A. GUVAKOVA AND EWA SURMACZ¹

Kimmel Cancer Institute, Thomas Jefferson University, Philadelphia, Pennsylvania 19107

INTRODUCTION

The insulin-like growth factor I receptor (IGF-IR) paracrine or autocrine loop plays an important role in the maintenance of breast cancer growth. Cancer cells contain several-fold higher levels of the IGF-IR than normal breast tissue; however, it is still not clear whether abnormally high activation of IGF-IR signaling may induce progression of the disease. To address this question, we have established several MCF-7-derived clones (MCF-7/IGF-IR cells) overexpressing the IGF-IR. We report here that overexpression of the IGF-IR did not modify sensitivity of cells to IGF-I; however, responsiveness to the ligand was moderately enhanced in most of the MCF-7/IGF-IR clones (measured by [³H]-thymidine incorporation into DNA). All MCF-7/IGF-IR clones responded to the synergistic action of 1 nM estradiol (E2) and small amounts of IGF-I (up to 0.8 ng/ml). Exposure of cells to higher concentrations of IGF-I abolished estrogen requirements for stimulation of DNA synthesis in all MCF-7/IGF-IR clones, but not in the parental cells. The most important finding of this work was that the amplification of the IGF-IR induced cell–cell adhesion in MCF-7 cells. High levels of the IGF-IR promoted cell aggregation on Matrigel, allowed proliferation of cells within the aggregates, and protected clustered cells from death. In both MCF-7 and MCF-7/IGF-IR cells, IGF-I stimulated aggregation, whereas an anti-E cadherin antibody blocked cell–cell adhesion. Furthermore, immunofluorescence staining with specific antibodies revealed co-localization of the IGF-IR and E-cadherin at the points of cell–cell contacts. Moreover, the IGF-IR and its two substrates, insulin receptor substrate 1 and SHC, were contained within the E-cadherin complexes. Our results suggest that overexpressed IGF-IRs, by promoting the aggregation, growth, and survival of breast cancer cells, may accelerate the increase of tumor mass and may also prevent cell scattering. © 1997 Academic Press

The insulin-like growth factor I receptor (IGF-IR)² belongs to the tyrosine kinase receptor superfamily [1]. Upon ligand binding, the intrinsic tyrosine kinase of the IGF-IR is activated, which results in the immediate tyrosine phosphorylation of several cellular substrates. Two well-characterized substrates are insulin receptor substrate-1 (IRS-1) and SHC [2–5]. Both act as docking proteins, recruiting different effector molecules and activating multiple signaling systems, for instance, the pathways of Ras or PI-3 kinase. Ultimately, some of the IGF-IR-induced signals stimulate nuclear events, while others are involved in the reorganization of cell morphology [2–9].

Several lines of evidence support an important role of the IGF system (the IGF-IR, its ligands, and IGF-binding proteins) in breast cancer. IGF-I and IGF-II are potent mitogens for cultured breast cancer cells [10] and the levels of the IGF-IR are significantly higher in breast tumors than in normal breast tissue [11]. In primary breast cancer, a correlation has been found between tumor size, the levels of IRS-1, and recurrence of the disease [12]. In estrogen-responsive breast cancer cells, physiological concentrations of estradiol (E2) upregulate the expression of IGF-IRs [13, 14], IGF-II [15], and certain binding proteins [16]. On the other hand, overexpression of IGF-II or IRS-1 renders cells estrogen-independent [14, 17]. Most importantly, blockade of the IGF-IR autocrine or paracrine loop with anti-IGF-IR antibodies, excess of IGF-binding protein, antisense RNA against IGF-IR, or antisense oligonucleotides against IRS-1 inhibits breast cancer growth *in vitro* or *in vivo* [14, 18–20].

The role of the IGF-IR in the metastasis of mammary tumor is not clear. In mouse mammary carcinoma, cells

¹To whom correspondence and reprints requests should be addressed at Kimmel Cancer Institute BLSB 606A, Thomas Jefferson University, 233S 10th Street, Philadelphia, PA 19107. Fax: (215) 923-0249.

²Abbreviations used: E2, 17- β -estradiol; FACS, fluorescence-assisted cell sorting; IGF-I, insulin-like growth factor I; IGF-IR, IGF-I receptor; IRS-1, insulin receptor substrate 1; MCF-7/IGF-IR, MCF-7 cells overexpressing IGF-IRs; NS, statistically nonsignificant; PCR, polymerase chain reaction; SFM, serum-free medium; PRF-SFM, phenol red-free SFM.

with higher levels of IGF-IRs are more metastatic [21]. On the other hand, based on the studies on IGF-IR content in breast tumors, it has been postulated that higher levels of the receptor are associated with a more favorable clinical outcome and may reflect a more differentiated breast cancer phenotype [11].

It is well established that in breast cancer cells, the acquisition of a metastatic phenotype may be related to deterioration or deactivation of adherens-type cell junctions. These types of junctions are structured around transmembrane cadherin proteins [22–26]. The strength of cadherin-mediated adhesion is regulated by different cytoplasmic catenins which connect cadherins to the actin filament network [24]. E-cadherin is often expressed in breast epithelial cells [22–24] and its presence usually correlates with a nonmetastatic phenotype [23–25]. On the other hand, loss or downregulation of E-cadherin has been observed in several metastatic breast cancer cell lines [23–25]. In several studies, restoration of E-cadherin function, by overexpression of this molecule or by treatment with growth factors or other compounds, resulted in increased adhesion and reduced metastasis [26–29]. Thus, an invasion suppressor role for E-cadherin has been postulated [28].

Here we report that in MCF-7 breast cancer cells, overexpressed IGF-IRs reduce estrogen requirements for growth and enhance responsiveness to low concentrations of IGF-I in the presence of E2. We also demonstrate that high levels of the IGF-IR promote cell–cell adhesion, allow proliferation of cells within aggregates, and protect clustered cells from death.

MATERIALS AND METHODS

IGF-IR expression plasmid. The pcDNA3/IGF-IR expression vector contains a full human IGF-IR cDNA [1] cloned into *Xho*–*Xba* polylinker sites of the pcDNA3 expression plasmid (Invitrogen). The expression of IGF-IR cDNA is driven by the CMV promoter. The plasmid also encodes a neomycin resistance gene.

Development of cell lines and cell culture conditions. MCF-7 cells were routinely grown in DMEM:F12 (1:1) containing 5% CS. In experiments that required estrogen-free conditions, cells were cultured in phenol red-free DMEM containing 0.5 mg/ml BSA, 1 μ M FeSO₄, and 2 mM L-glutamine (PRF-SFM).

The MCF-7/IGF-IR cell lines used in this study were developed by stable transfection with plasmids pcDNA3/IGF-IR or pcDNA3, followed by selection in medium containing 2 mg/ml G418. The neomycin-resistant clones were then screened by PCR. MCF-7/IGF-IR clones were maintained in culture for no longer than 3 months in the above medium with addition of 200 μ g/ml G418.

PCR. The incorporation of the IGF-IR cDNA into MCF-7 cells' genome was assessed by PCR. Briefly, DNA was isolated from 1000 to 10,000 cells. A fragment of the IGF-IR DNA was amplified using the following primers: upstream primer (located in the exon I of the IGF-IR coding sequence) 5'-AAG GAA TGA AGT CTG GCT CC-3'; downstream primer 5'-CTC GAT CAC CGT GCA GTT CT-3' (in exon II). Using these primers we were able to discriminate between the endogenous and the transfected IGF-IR DNAs. The conditions of PCR were 35 cycles of denaturation at 94°C for 1 min, annealing at

55°C for 1 min, extension at 72°C for 1 min; the last extension was for 6 min. The size of the DNA fragment amplified from the transfected IGF-IR cDNA was 170 bp.

FACS. To estimate the level of the IGF-IR in each of the MCF-7/IGF-IR clones, we used fluorescence-activated flow cytometry sorting (FACS) [30]. Briefly, the cells were cultured for 3 days in PRF-SFM (to downregulate endogenous receptors). Then the cells were trypsinized, washed with ice-cold PBS, and incubated for 30 min at 4°C in PBS containing 10 μ g/ml of an anti-IGF-IR antibody (alpha-IR3, Oncogene Science). Next, the cells were washed with ice-cold PBS and incubated in the dark for 30 min at 4°C with 2 μ g/ml of an FITC-conjugated goat anti-mouse IgG (Oncogene Science). Unbound antibody was removed by washing with PBS and the level of fluorescence was determined with EPICS Profile Analyzer. The primary antibody was omitted in control experiments.

Scatchard analysis. The number of the IGF-IR and ligand/receptor dissociation constant was determined by ligand replacement assay [30]. Briefly, the cells were plated at 1×10^5 cells per well in a 12-well plate in DMEM:F12 containing 5% CS. Next day, the cells were shifted to PRF-SFM for 3 days. Then, the cells were washed with DMEM and incubated for 6 h at 4°C in binding buffer [30] containing 0.1 nM ¹²⁵I-IGF-I (NEN/DuPont) and increasing concentrations of unlabeled IGF-I (at a range 0.0–5.0 nM). Next, the cells were washed three times with PBS containing 1 mg/ml BSA and lysed with 0.03% SDS. Cell-bound radioactivity was measured using a gamma counter. Nonspecific binding was determined in the presence of 33.0 nM unlabeled IGF-I. The binding characteristic was analyzed by the LIGAND program. For all tested cell lines, the best fit of binding was obtained with a one-site model.

Binding competition assay. The IGF-I binding assay was performed in the presence of insulin [31]. The cells were plated and synchronized in SFM as described for Scatchard analysis and then incubated with 0.1 nM ¹²⁵I-IGF-I and unlabeled insulin at concentrations from 0.01 to 100 nM. The same amounts of unlabeled IGF-I were used in control experiments. The amount of cell-bound ¹²⁵I-IGF-I was determined as described above.

Western blotting and immunoprecipitation. The levels of IGF-IR, IRS-1, SHC, and E-cadherin, as well as the levels of tyrosine phosphorylation of these proteins, were measured by Western blotting. The cells were cultured as described in the figure legends and then lysed, as described in Refs. [30, 32]. The protein lysate (300–1000 μ g) was immunoprecipitated with an appropriate antibody. The following antibodies were used for immunoprecipitation: for IGF-IR, an anti-IGF-IR monoclonal antibody alpha-IR3 (Oncogene Science); for IRS-1, an anti-IRS-1 polyclonal antibody (UBI); for SHC, an anti-SHC polyclonal antibody (Transduction Laboratories); and for E-cadherin, an anti-E-cadherin monoclonal antibody (Transduction Laboratories). The immunoprecipitates were resolved by PAGE and the proteins were immunodetected with the appropriate antibody. For IRS-1, SHC, and E-cadherin, the antibodies were the same as used for immunoprecipitation. To detect the IGF-IR, we used an anti-IGF-IR polyclonal antibody (Santa Cruz). Tyrosine phosphorylation of the above proteins was detected by immunoblotting with an anti-phosphotyrosine monoclonal antibody PY20 (Transduction Laboratories). The amounts of proteins were estimated by laser densitometry reading. Tyrosine phosphorylation level of E-cadherin-associated proteins was measured 72 h after stimulation (which was the time necessary to complete and stabilize cell–cell aggregation).

[³H]Thymidine incorporation. Cells were plated into 96-well plates at a concentration of 1×10^4 cells per well in DMEM:F12 containing 5% CS and were grown until 80% confluent. Then, the medium was replaced with PRF-SFM containing 10 nM tamoxifen (to synchronize the cells in quiescence). After 3 days, the cells were washed twice with PRF-SFM and incubated in PRF-SFM supplemented with different amounts of IGF-I, E2, or IGF-I + E2 for 18–20 h. Next, the cultures were pulsed with 0.5 μ Ci/well of [³H]-thymidine for 4 h. The amount of radioactivity incorporated into

trichloroacetic acid-insoluble material was counted using a beta counter (1209 Rackbeta, Wallac). The stimulation of [³H]thymidine incorporation into DNA was calculated as follows: cpm's obtained in unstimulated cells (PRF-SFM) were taken as basal value equaling 100%; cpm's in cells stimulated with either IGF-I, E2, or IGF-I + E2 were expressed as the percentage increase over basal level.

The sensitivity index ED₅₀ was calculated as described in Ref. [33].

Soft agar assay. The anchorage-independent growth was determined by soft agar assay as described previously [14]. The growth of cells was tested in semisolid DMEM:F12 medium supplemented with either 10 or 2% FBS, as well as in PRF-SFM supplemented with 200 ng/ml IGF-I. Colonies of a size greater than 150 μm were counted after 2 and 3 weeks.

Aggregation on Matrigel. Matrigel (Biocoat/Fisher) was reconstituted according to the manufacturer's instructions. The matrix (200 μl/well) was placed in a 24-well plate and allowed to solidify. A cell suspension of 2 × 10⁴ cells in DMEM:F12 plus 5% CS was plated in each well and cultured for up to 21 days. The cultures were photographed at Days 5 and 11. At Day 16, the cells were released from the matrix using Dispase (Biocoat/Fisher), stained with trypan blue, and counted in a hemocytometer.

In several experiments, the cells were cultured on Matrigel in the presence of 50 ng/ml IGF-I to assess the ligand-dependent increase of aggregation. The requirement for E-cadherin was tested with the anti-E-cadherin antibody HECD-1 (Zymed) which was added at the time of plating at a concentration of 10 μg/ml.

Invasion assay. The invasiveness of MCF-7/IGF-IR cells was studied using 24-well invasion chambers (Biocoat/Fisher). Cells (2 × 10⁴) suspended in DMEM:F12 with 5% CS were placed in the upper chamber and cultured for 24 or 48 h. Lower chambers contained the same growth medium. The number of cells that invaded the extracellular matrix and migrated to the underside of the chamber was determined by direct counting (after staining with 0.5% crystal violet). In several experiments, the medium in the lower chamber was supplemented with IGF-I (50–200 ng/ml) or E2 (10 nM) used as chemoattractants.

Immunofluorescence microscopy. The double staining for the IGF-IR and E-cadherin was performed on monolayer cultures of MCF-7 and MCF-7/IGF-IR cells. The localization of the IGF-IR was detected using indirect immunofluorescence, as recommended by Transduction Laboratories (protocol 9). Briefly, 70% confluent cells grown on glass coverslips were fixed for 10 min at room temperature (RT) in 3.7% formaldehyde, washed with PBS, treated with 0.2% Triton X-100 for 5 min, and then blocked in 0.2% BSA for 5 min. The fixed cells were incubated for 1 h at RT with 10 μg/ml of a rabbit polyclonal anti-human IGF-IR antibody (Santa Cruz), washed with PBS, and incubated with an anti-rabbit-lissamine/rhodamine-conjugated goat IgG (26 μg/ml) for 30 min. The localization of E-cadherin determined on the same slides using a monoclonal antibody HECD-1 (10 μg/ml) and a goat anti-mouse IgG-FITC-conjugated (2 μg/ml). The primary antibodies were omitted in control experiments.

Statistical analysis. The statistical evaluation of results was done using ANOVA single-factor analysis of variance. The significance level was taken as $P \leq 0.05$.

RESULTS

Development of MCF-7/IGF-IR clones. The MCF-7/IGF-IR clones were developed by stable transfection of MCF-7 cells with the pcDNA3/IGF-IR expression vector. The transfected cells were selected in 2 mg/ml G418. Forty-four G418-resistant clones were analyzed by PCR to detect the cells with the integrated IGF-IR plasmid and by FACS to identify the clones that

overexpressed the IGF-IR. Ultimately, five MCF-7/IGF-IR clones were obtained, designated C-12, C-34, C-21, C-17, and C-15. In parallel, by stable transfection of MCF-7 cells with the pcDNA3 vector, we generated control clones MCF-7/pc 2 and MCF-7/pc 4.

The number of IGF-I receptors in MCF-7/IGF-IR clones was determined by Scatchard analysis (Fig. 1B). The cells were incubated for 4 days in phenol red-free serum-free medium (PRF-SFM) to ensure downregulation of endogenous IGF-IRs in the absence of E2. The IGF-IR content in MCF-7/IGF-IR clones ranged from 0.5 × 10⁶ to 3.0 × 10⁶ receptors/cell, which represented an 8- to 50-fold increase over the IGF-IR level in MCF-7 cells (0.6 × 10⁵ receptors/cell) [14] (Figs. 1A and B). The number of receptors in the control MCF-7/pc 2 and pc 4 clones was slightly lower than that in the parental cells (0.3 × 10⁵ and 0.4 × 10⁵ sites/cell, respectively) but the differences did not reach statistical significance. The dissociation constant (K_d) in all clones was in the range of K_d values reported for IGF-I/IGF-IR binding [34–36] (Fig. 1A). In addition, in order to rule out the possibility that the increased number of binding sites was due to selective formation of IGF-I/insulin hybrid receptors [31], binding competition assays with insulin were performed. In the all MCF-7/IGF-IR clones, IGF-I binding was not displaced even with very high (100 nM) concentrations of insulin (data not shown).

Figure 1C demonstrates the IGF-IR levels in MCF-7/IGF-IR clones by FACS. Compared with MCF-7 cells, the increase in relative IGF-IR fluorescence in MCF-7/IGF-IR clones was from 2.5- to 25.1-fold. MCF-7/pc 2 and pc 4 clones exhibited fluorescence similar to that in MCF-7 cells (0.9 and 0.95 of the level in the parental cells).

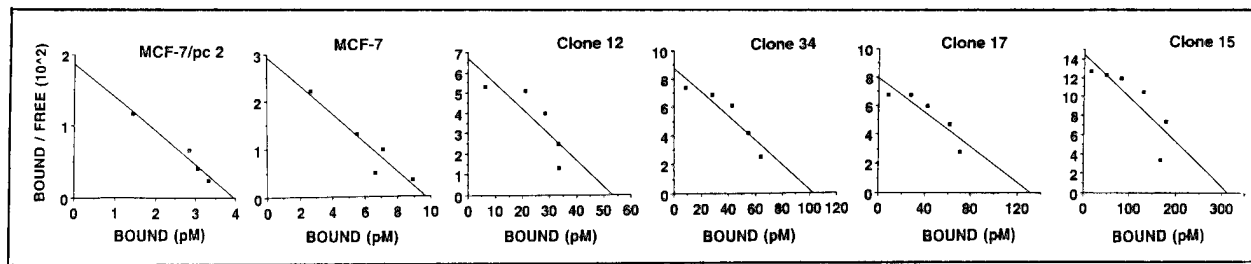
Additionally, the level of the IGF-IR protein in the developed clones was assessed by immunoprecipitation and subsequent immunoblotting with an anti-IGF-IR antibody (Fig. 2A). The increase of the IGF-IR beta-subunit in the clones C-12, C-34, C-21, C-17, and C-15 compared with that in MCF-7 cells was 2-, 5-, 7-, 10-, and 21-fold, respectively (estimated by laser densitometry). The levels of IGF-IR protein in clones MCF-7/pc 2 and pc 4 were similar to those in MCF-7 cells and were barely detectable by Western blotting (not shown).

In MCF-7/IGF-IR clones, both basal and IGF-I-induced tyrosine phosphorylation of the IGF-IR and IRS-1 were markedly increased compared with the levels in the parental cells. The representative experiment, involving clones with the highest overexpression of the receptor, is shown in Fig. 2B. In MCF-7/IGF-IR clones 15 and 17, the levels of tyrosine phosphorylation of the IGF-IR were consistently at least 4-fold higher in cells treated for 5 min with IGF-I, and at least 8-fold higher under SFM, than the corresponding levels in MCF-7

A

Cells	MCF-7/pc 2	MCF-7	Clone 12	Clone 34	Clone 21	Clone 17	Clone 15
N_R	0.03×10^6	0.06×10^6	0.5×10^6	0.9×10^6	0.8×10^6	1.1×10^6	3.0×10^6
K_d	0.21	0.28	0.79	1.16	0.47	1.65	2.1
K_{FACS}	0.9	1.0	2.5	2.8	6.9	12.6	25.1

B



C

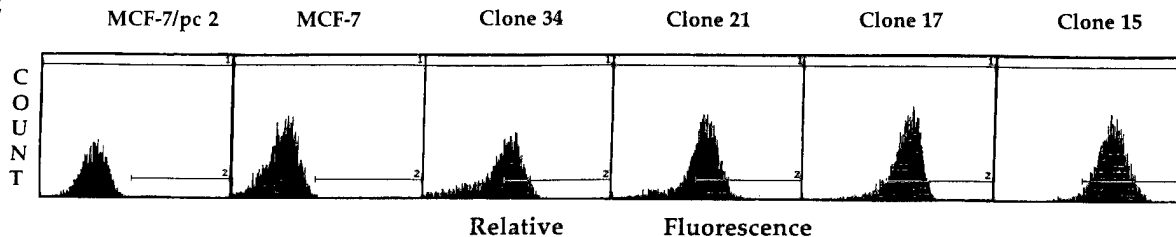


FIG. 1. Characteristics of MCF-7/IGF-IR clones. (A) Summary of parameters: IGF-IR number (N_R), dissociation constant K_d (nM), and relative fluorescence index (K_{FACS}). Binding parameters were determined, and FACS analysis was performed, as described under Materials and Methods. K_{FACS} represents the fold increase of the relative IGF-IR fluorescence in MCF-7/IGF-IR clones over that in MCF-7 cells. (B) Scatchard analysis. Abscissa, bound IGF (pM); ordinate, bound/free IGF $\times 10^{-2}$. The binding experiments for each clone were repeated at least three times. The representative Scatchard plots are shown. (C) FACS analysis. Abscissa, relative IGF-IR fluorescence; ordinate, cell number. In each experiment, 5×10^3 of cells were analyzed. Each analysis was performed at least two times. The representative results are shown. In control experiments, where cells were stained with secondary antibody only, the level of fluorescence was undetectable.

cells (estimated by laser densitometry). The tyrosine phosphorylation of IRS-1 was also more pronounced in MCF-7/IGF-IR clones than in the parental cells: specifically, at least 2-fold greater under IGF treatment, and from 1.6- (clone 12) to 6-fold (clone 15) greater in SFM (Fig. 2C). In the latter case, presumably due to a low concentration of ligand, there was an apparent correlation between tyrosine phosphorylation of IRS-1 and the number of IGF-IRs. In the presence of IGF-I, the saturation of IRS-1 stimulation was obtained in clone 12 expressing 5×10^6 receptors/cell. The levels of IRS-1 protein in the studied cells were similar under all experimental conditions (not shown).

E2 responsiveness in MCF-7/IGF-IR cells. MCF-7 cells and all developed MCF-7/IGF-IR clones responded similarly to E2 with stimulation of [3 H]thymidine incorporation into DNA (data not shown). In all cell lines, 0.05 nM E2 yielded a maximal response (a 2.9- to 6.8-fold increase over the basal level), while concentrations

up to 1.0 nM had no additional effect. The differences in E2 responsiveness observed among the tested clones were not statistically significant. E2 at a concentration higher than 20.0 nM exerted an inhibitory effect. Consequently, a concentration of 0.1 nM E2 was used in all further experiments.

Sensitivity and responsiveness of MCF-7/IGF-IR cells to IGF-I alone or in combination with E2. The overexpression of IGF-IR did not modify sensitivity to IGF-I (evaluated by [3 H]thymidine incorporation into DNA) (Fig. 3). Specifically, the ED_{50} for MCF-7 was 0.56 ng/ml and for MCF-7/IGF-IR cells it ranged from 0.42 to 0.67 ng/ml, $P = NS$. The responsiveness to IGF-I, however, was increased in most MCF-7/IGF-IR clones. For instance, with 4 ng/ml IGF-I, there was a 325% increase of [3 H]thymidine incorporation in MCF-7 cells, whereas increases of 336, 492, 580, 728, and 648% were observed in clones C21, C12, C34, C17, and C15, respectively.

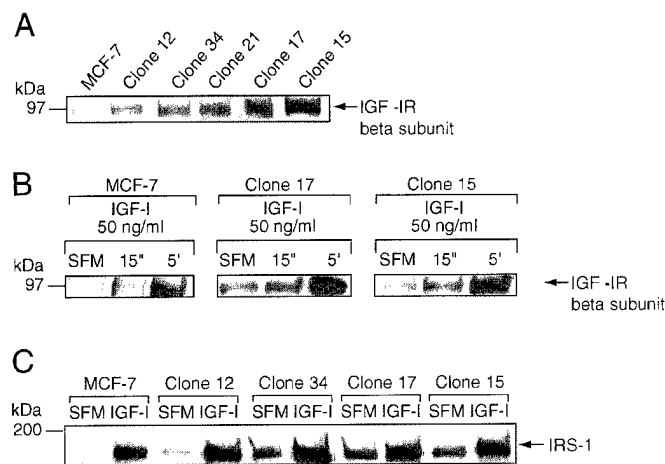


FIG. 2. Activation of IGF-IR signaling in MCF-7/IGF-IR cells. (A) IGF-IR protein levels. The IGF-IR protein level in MCF-7 cells and clones 12, 34, 21, 17, and 15 was determined by immunoprecipitation with an anti-IGF-IR antibody and subsequent Western immunoblotting, as described under Materials and Methods. 300 μ g and 1 mg of proteins were used to immunoprecipitate the IGF-IR from MCF-7/IGF-IR and MCF-7 cells, respectively. The analysis was performed at least two times for each clone. (B) Tyrosine phosphorylation of the IGF-IR. Cells were incubated in PRF-SFM for 3 days and then stimulated with 50 ng/ml IGF-I for 15 s or 5 min. Tyrosine phosphorylation of the IGF-IR was measured by immunoprecipitation with an anti-IGF-IR antibody followed by Western immunoblotting with an anti-phosphotyrosine antibody. The experiments were repeated at least four times; representative results for MCF-7 cells, clone 17, and clone 15 are shown. (C) Tyrosine phosphorylation of IRS-1. Cells were grown in PRF-SFM for 3 days with or without 50 ng/ml of IGF-I. 300 μ g of lysate was immunoprecipitated with an anti-IRS-1 antibody and immunoblotted with an anti-phosphotyrosine antibody. The experiments were repeated at least two times; representative results are presented.

In MCF-7 cells, 0.1 nM E2 combined with IGF-I (0.01–100 ng/ml) produced a synergistic effect on [³H]-thymidine incorporation. In contrast, in all MCF-7/IGF-IR clones, E2 increased the mitogenic response only in the presence of low concentrations of IGF-I (less than 1 ng/ml). With larger amounts of IGF-I, the synergistic effect of E2 was abolished, and IGF-I alone was sufficient to maximally stimulate DNA synthesis (Fig. 3). The effect of IGF-I alone or in combination with E2 on DNA synthesis in MCF-7/pc clones was similar to that found for MCF-7 cells (not shown).

Overexpression of the IGF-IR does not improve the ability of MCF-7 cells to grow in soft agar or in monolayer culture. The ability of MCF-7/IGF-IR clones to grow under anchorage-independent conditions was similar to that exhibited by MCF-7 and MCF-7/pc cells. Specifically, all tested cell lines formed approximately 100 colonies in soft agar containing 10% FBS, 120 colonies in agar with 10% FBS plus 200 ng/ml IGF-I, and 45 colonies in agar with 2% FBS. In addition, similarly to the parental cell line, none of the MCF-7/IGF-IR

cells produced colonies greater than 100 μ m in semi-solid PRF-SFM supplemented with 200 ng/ml IGF-I.

In monolayer culture, the increase in cell number was similar in all studied cell lines, regardless of the level of IGF-IR overexpression. Specifically, 72 h after stimulation with IGF-I (0.1–10 ng/ml), in all cases, the number of cells increased $\sim 1.7 \pm 0.3$ -fold (data not shown).

Overexpression of the IGF-IR does not induce invasiveness of MCF-7 cells in vitro. MCF-7 cells have been reported as noninvasive or poorly invasive [27]. We found that the overexpression of IGF-IR in MCF-7 cells did not alter their noninvasive phenotype *in vitro*. Using invasion chambers (Biocoat/Fisher), we noted that only approximately 0.2% cells were able to traverse the extracellular matrix. Additionally, invasiveness of the cells was not stimulated when IGF-I or the combination of IGF-I + E2 was used as chemoattractant.

Overexpression of the IGF-IR stimulates cell-cell adhesion in MCF-7 cells. MCF-7 cells cultured on Matrigel (extracellular matrix) formed globular aggregates characteristic of a noninvasive phenotype [27]. As shown in Fig. 4, cell aggregation was significantly stimulated in clones overexpressing the IGF-IR. The extent of aggregation appeared to parallel the increase of the IGF-IR number in the cells (Figs. 4a–4e). For instance, at Day 5 of culture, MCF-7 cells did not produce any aggregates of a size greater than 150 μ m, whereas the clones C-12 and C-34 (Figs. 4b and 4c) formed an average of 8 and 10 such aggregates, respectively. The clones 17 and 15 (Figs. 4d and 4e) produced a few clusters of a size greater than 300 μ m and several smaller aggregates of the size 150–300 μ m. The average results from five experiments were as follows: for clone C-17, there were 4 aggregates greater than 300 μ m and 5 of the size 150–300 μ m, and for clone 15, there were aggregates greater than 300 μ m and 7 of the size 150–300 μ m.

When culture on Matrigel was extended up to 21 days, MCF-7 cells and the clones expressing less than 1.1×10^6 IGF-IRs progressively disaggregated and died (Fig. 4f–4h). At Day 16 of the experiment, of 2×10^4 initially plated cells, we found an average of 1.2×10^2 , 1×10^2 , and 8×10^3 viable cells for MCF-7, clone 34, and clone 12, respectively. In contrast, the clones expressing the highest levels of the IGF-IR not only remained well aggregated, but also proliferated in compact clusters (Figs. 4i–4j). Indeed, at Day 16, the number of cells was even increased up to 1.1×10^5 cells for clone 17 and to 4.6×10^4 cells for clone 15.

The aggregation and survival of MCF-7/pc 2 and pc 4 cells cultured on Matrigel was similar to that noted for the parental cells. The morphology and size of the clusters produced by MCF-7/pc 2 cells is shown in Fig. 5A.

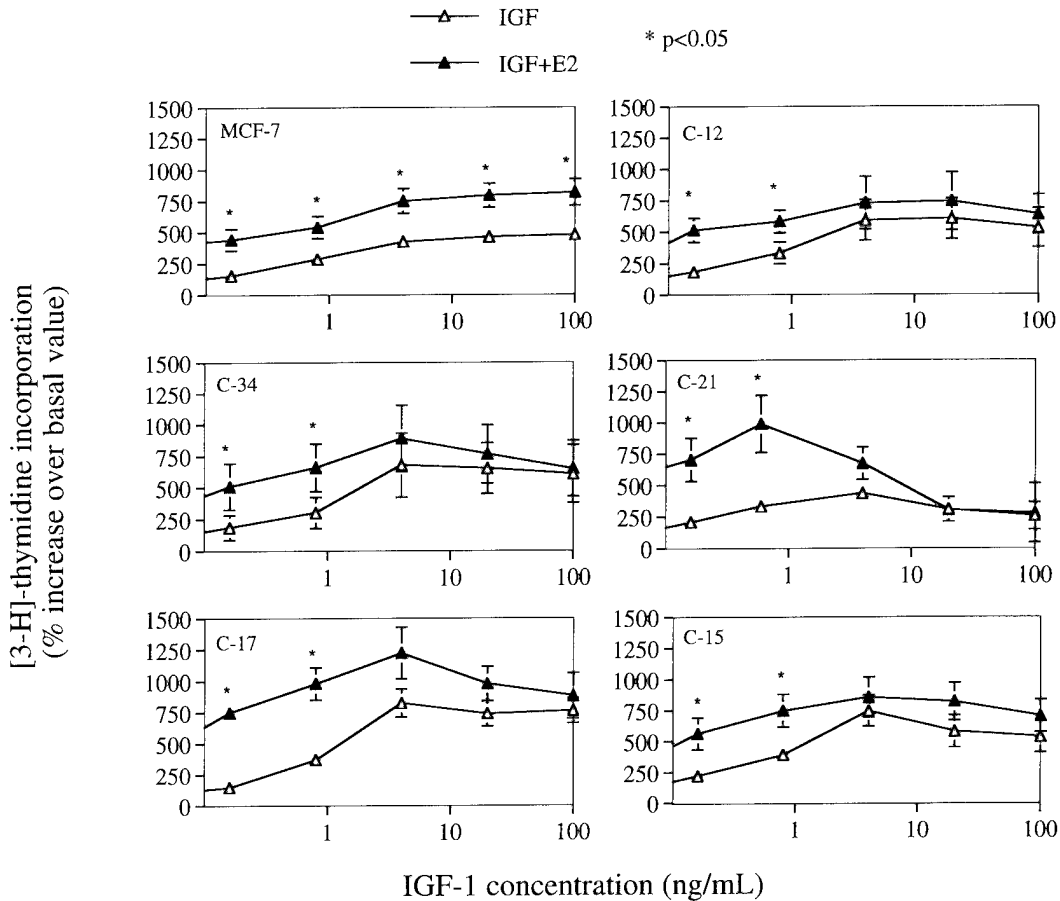


FIG. 3. Stimulation of [³H]thymidine incorporation by IGF-I alone or in combination with E2 in MCF-7 and MCF-7/IGF-IR cells. The cells were synchronized and stimulated with different amounts of IGF-I with or without 0.1 nM E2, as described under Materials and Methods. Abscissa, tested concentrations of IGF-I. Ordinate, percentage increase of [³H]thymidine incorporation (in cpm) over basal level (cpm values in untreated cells). The values are means from at least four experiments. Bars, SE. Asterisks indicate statistically significant differences between IGF-I and IGF-I plus E2 values by ANOVA ($P < 0.05$).

IGF-I stimulates aggregation of MCF-7 and MCF-7/IGF-IR cells: Anti-E-cadherin antibody blocks the formation of aggregates. In the presence of 20 ng/ml IGF-I, MCF-7 cells as well as MCF-7/IGF-IR clones displayed increased aggregation on Matrigel. As shown in Fig. 5, the size of average aggregates typically increased from approximately 100 to 150 μ m in MCF-7 cells (Fig. 5B, parts a and c), and from 180 to 250 μ m in clone 15 (Fig. 5B, parts b and d). In contrast, in all studied cell lines, the addition of an anti-E-cadherin antibody at the time of cell plating effectively blocked cell-cell adhesion. The effect of anti-E-cadherin antibody on aggregation in MCF-7 cells and in MCF-7/IGF-IR clone 15 is presented in Fig. 5B, parts e and f.

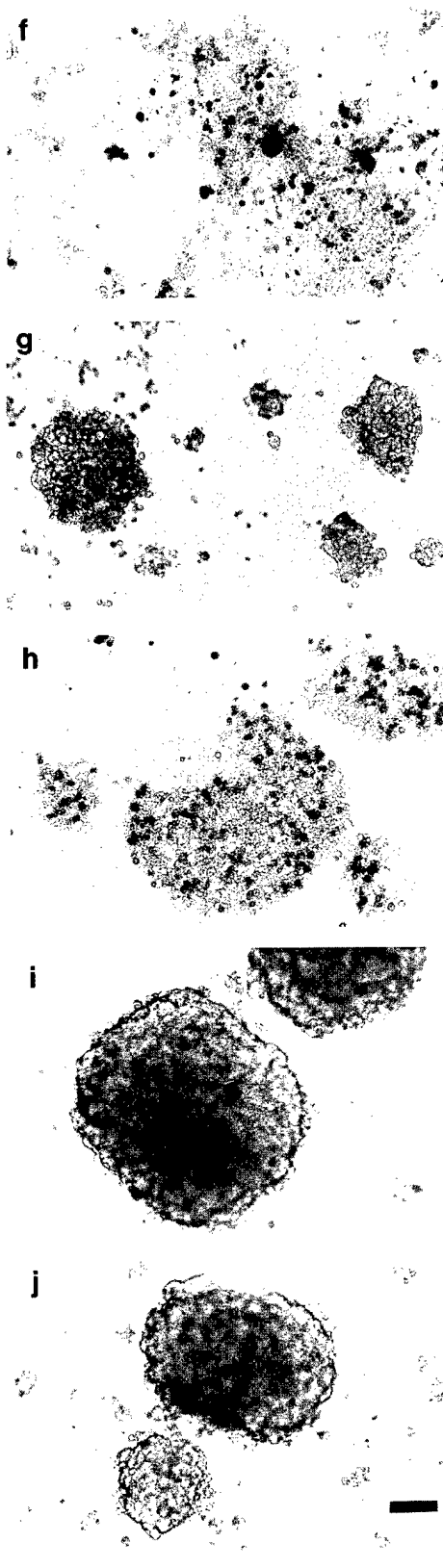
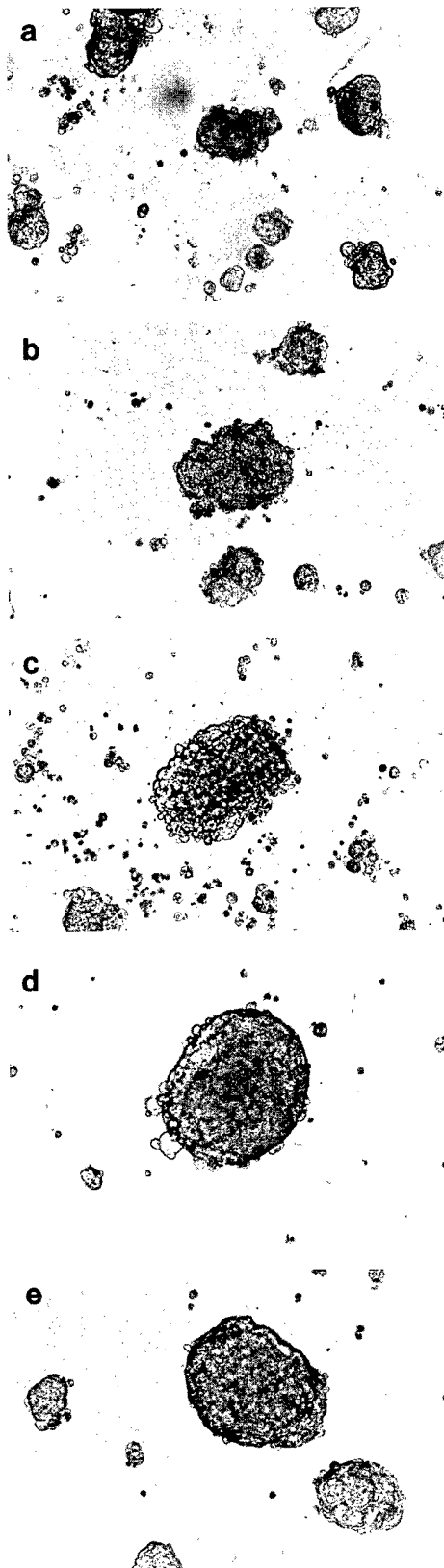
The IGF-IR co-localizes with E-cadherin in MCF-7/IGF-IR cells. The IGF-IR and E-cadherin were detected by double-staining with specific antibodies. In MCF-7 cells, immunofluorescence analysis with an anti-IGF-IR antibody produced barely visible staining on the cell surface (Fig. 6a), while immunodetection with anti-E-cadherin antibody revealed the typical E-cadherin honeycomb pattern [25] (Fig. 6b).

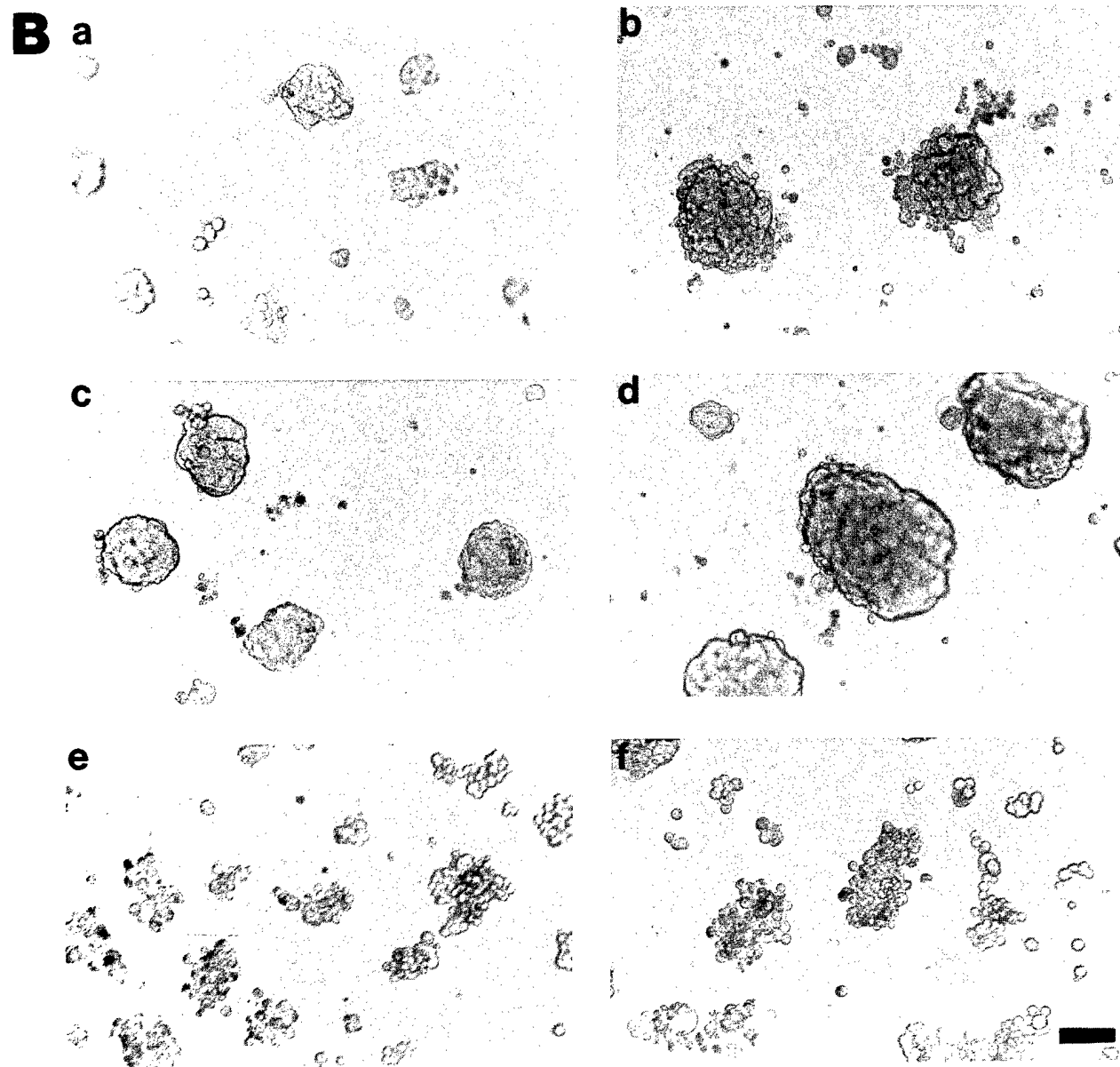
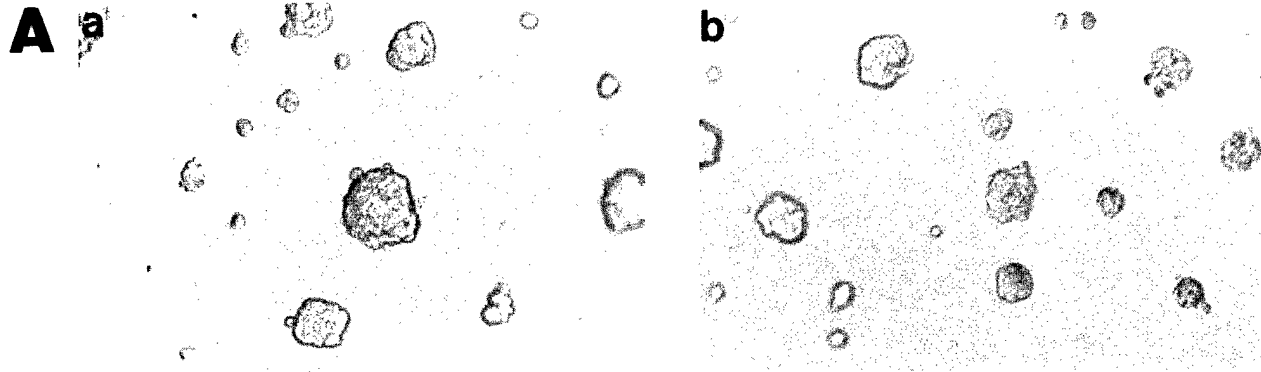
In MCF-7/IGF-IR clones, the IGF-IR was easily detectable by immunofluorescence. The staining appeared to be concentrated at areas of cell-cell contacts (Figs. 6c and 6e), which was particularly evident in clones with very high receptor content (Fig. 6e). Remarkably, in MCF-7/IGF-IR clones, the IGF-IR co-lo-

FIG. 4. Aggregation of MCF-7/IGF-IR cells. 20,000 cells were plated on Matrigel. The morphology of the clones was recorded by phase-contrast microscopy after 5 and 11 days of culture. MCF-7 cells (a, f); clone 12 (b, g); clone 34 (c, h), clone 17 (d, i); clone 15 (e, j). Bar, 100 μ m. The experiments were repeated at least four times for all analyzed cells. The representative results are shown.

Day 5

Day 11





calized with E-cadherin (Figs. 6d and 6f). Interestingly, in contrast to the uniform membrane distribution of E-cadherin in MCF-7 cells, the localization of this protein appeared to be altered in cells with very high IGF-IR content. Specifically, more E-cadherin tended to accumulate in the areas of cell membranes containing the highest amounts of the IGF-IR (Figs. 6e and 6f).

IGF-IR, IRS-1, and SHC associate with E-cadherin.

We further investigated whether the IGF-IR and associated substrates physically interact with E-cadherin complexes. Figure 7 shows representative data from several independent experiments. Figure 7A demonstrates patterns of tyrosine phosphorylation of proteins coprecipitating with E-cadherin in MCF-7 cells and in clones 12, 17, and 15 cultured under various conditions. In all analyzed cells, the patterns of tyrosine phosphorylated proteins associated with E-cadherin were similar (Fig. 7A) and contained at least seven distinct bands. The most prominent were the bands of the approximate sizes 95, 185, and 200 kDa (the last not seen in MCF-7 cells). In the following experiments, we examined, by reprobing the blots with different antibodies, whether E-cadherin-associated proteins contain the elements of the IGF-I signaling pathway. Due to multiple stripping and reprobing, we were not always able to demonstrate the levels of all studied proteins in each individual blot. However, in several independent experiments, we confirmed the presence of each of the IGF-IR signaling molecules, the IGF-IR, IRS-1, and SHC, in E-cadherin complexes of all studied cells (not shown).

Figure 7B demonstrates the amounts of E-cadherin, IRS-1, IGF-IR, or SHC in the precipitates. E-cadherin, as expected, was detectable in all precipitates. In MCF-7 cells, a 185-kDa band noticeable in cells treated with IGF-I (Fig. 7A) contained IRS-1. IRS-1 was also present in E-cadherin precipitates of other cells (shown here for clone 15). In contrast to MCF-7 cells, however, tyrosine phosphorylation of IRS-1 in MCF-7/IGF-IR clones 12, 17, and 15 was also noticed under SFM or 5% CS conditions.

The E-cadherin complexes contained the IGF-IR (shown here for MCF-7 cells, clone 12, and clone 17). Relative to E-cadherin levels, the amount of IGF-IRs in the complexes appeared to be greater in cells overexpressing the receptor (see clones 12 and 17, compared with MCF-7 cells). The extent of tyrosine phosphorylation of the IGF-IR was impossible to determine since the phosphorylated band of the size 95 kDa contained

not only the IGF-IR but also large amounts of β -catenin which was phosphorylated on tyrosine residues (not shown).

The tyrosine phosphorylation of E-cadherin was low and was further reduced (approximately 50%) in MCF-7, clone 12, and clone 15, as a result of 72 h of IGF-I treatment (Fig. 7). In several experiments, we did not notice any consistent modification of E-cadherin protein expression under IGF-I. The exception was clone 17, in which IGF-I caused a reduction of E-cadherin levels.

SHC proteins complexed with E-cadherin were not phosphorylated on tyrosines under any of the experimental conditions.

DISCUSSION

Although numerous studies [10–20] have suggested an important role for the IGF paracrine or autocrine loop in the regulation of breast cancer growth, the impact of the IGF-IR on the progression of the disease is still largely unknown. Here, we examined whether a substantial increase in the IGF-IR levels would induce processes associated with breast cancer progression, such as increased sensitivity or responsiveness to IGF-I, development of estrogen independence, enhancement of anchorage-independent growth, or induction of invasiveness. In IGF-I- and E2-dependent, noninvasive MCF-7 cells, the overexpression of the IGF-IR produced: (i) a moderate mitogenic effect, reflected by sensitization of cells to low concentrations of IGF-I in the presence of E2 and reduction of E2 requirements with large amounts of IGF-I, and (ii) a marked morphogenic effect, reflected by stimulation of cell-cell adhesion.

Our studies were greatly facilitated by the successful development of MCF-7-derived clones expressing different levels of IGF-IRs. The first part of this work provides characteristics of our experimental model. The expression of IGF-IRs was determined by three independent methods: Scatchard binding assay (Fig. 1B), FACS analysis (Fig. 1C), and Western immunoblotting (Fig. 2). The number of IGF-I binding sites in the developed clones assessed by Scatchard assay was from 8- to 50-fold higher than that in the parental cells (Figs. 1A and 1C). This higher IGF-I binding was not associated with any noticeable overexpression of low-affinity binding sites for IGF-I (likely to represent surface IGF binding proteins [37] (Fig. 1B). Hybrid IGF-I/insulin receptors, with affinity toward both li-

FIG. 5. (A) Aggregation of a control clone. The morphology of control cells MCF-7 (a) and MCF-7/pc2 (b) at Day 5 of culture on Matrigel. Three independent experiments were performed. (B) Effects of IGF-I and anti-E-cadherin antibody on aggregation of MCF-7 and MCF-7/IGF-IR cells. The sizes and morphology of average aggregates produced by MCF-7 cells (a–e) and MCF-7/IGF-IR clone 15 (b–f) cultured in control medium were analyzed on Day 5 of the experiment. In parallel, the cells were grown in the presence of 50 ng/ml IGF-I (MCF-7, c; clone 15, d) or 10 μ g/ml of anti-E-cadherin antibody (HECD 1) (MCF-7, e; clone 15, f).

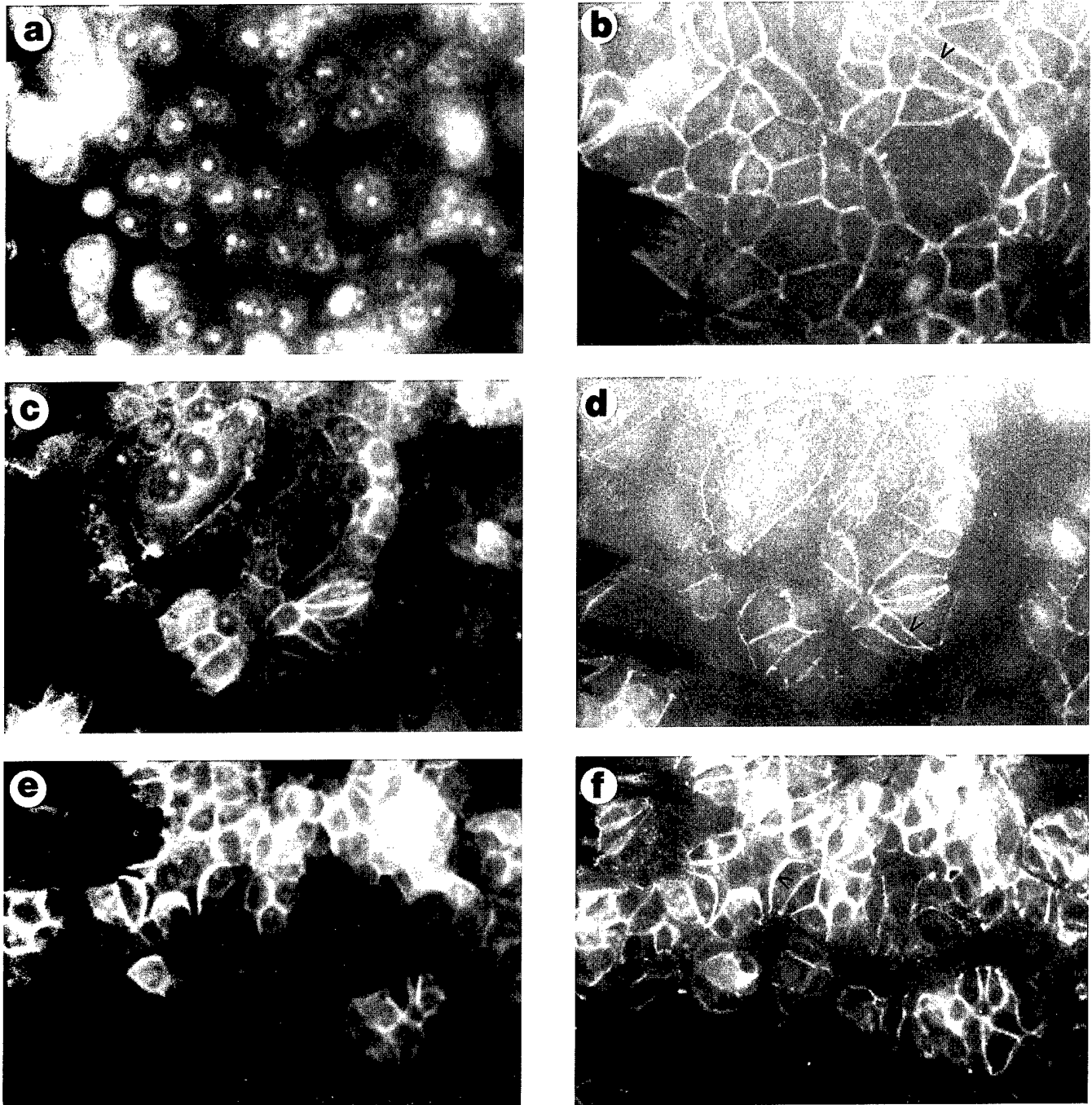


FIG. 6. Co-localization of the IGF-IR and E-cadherin in MCF-7/IGF-IR cells. The IGF-IR was detected with an anti-IGF-IR polyclonal antibody and anti-rabbit rhodamine-conjugated IgG. E-cadherin was localized with an anti-E-cadherin monoclonal antibody (HECD-1) and anti-mouse FITC-conjugated IgG, as described under Materials and Methods. The localization of the IGF-IR in MCF-7 cells (a), clone 12 (c), clone 15 (e) and the staining for E-cadherin in MCF-7 (b), clone 12 (d) and clone 15 (f) were examined and photographed under a Zeiss axiophot microscope with an original magnification of $\times 400$. The arrowheads indicate specific staining. The fluorescence staining observed in the cell nucleoli in a, c, and e was nonspecific.

gands, have been described in many models [31]. We established, by competition binding, that in the MCF-7/IGF-IR clones, IGF-I, but not insulin, was the principal ligand for the overexpressed receptors.

The overexpression of the IGF-IR in MCF-7/IGF-IR cells was further confirmed by two semiquantitative methods, FACS analysis and Western immunoblotting. By FACS, the amount of the IGF-IR protein in the

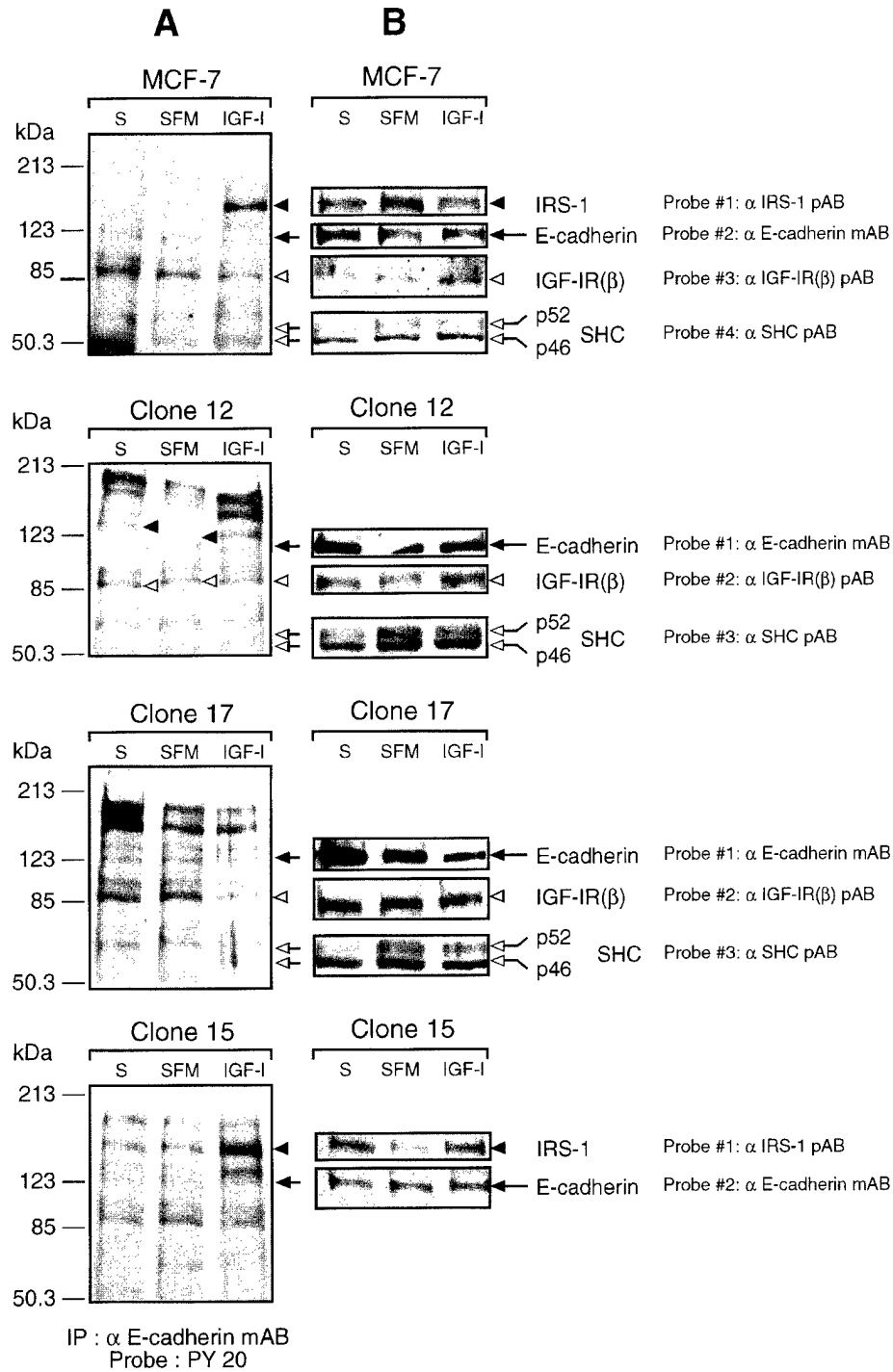


FIG. 7. Association of IGF-I signaling molecules with E-cadherin. Cells were incubated for 3 days in DMEM:F12 with 5% CS (S), PRF-SFM (SFM) or PRF-SFM with 50 ng/ml IGF-I (IGF-I) and then lysed. (A) Tyrosine phosphorylation of E-cadherin-associated proteins. 500 μ g of protein lysate was immunoprecipitated with 4 μ g of an anti-E-cadherin monoclonal antibody. (B) Protein levels of E-cadherin and associated proteins. The immunoblots shown in (A) were stripped and reprobed with an anti-E-cadherin antibody. Next, the membranes were stripped again and reprobed with either an anti-IRS-1 or an anti-IGF-IR antibody. Subsequently, the blots probed with an anti-IGF-IR antibody were stripped and hybridized with an anti-SHC antibody. Due to multiple stripping and the resulting decrease in membrane-bound proteins, we were not able to demonstrate the levels of all studied proteins in a single blot. Note: the E-cadherin and IGF-IR bands in the clone 12 blot were shifted because of a gel crack.

developed clones was elevated from 2.5- to 25.1-fold compared with MCF-7 cells (Fig. 1C); Western blotting revealed a 2- to 21-fold increase (Fig. 2A). Furthermore, we provided evidence that in MCF-7/IGF-IR cells, the extent of IGF-I-induced tyrosine phosphorylation of both IGF-IR and IRS-1 was higher than in MCF-7 cells. Interestingly, a saturation of IGF-stimulated tyrosine phosphorylation was observed. In the case of the receptor, the maximum was seen in cells expressing approximately 1×10^6 sites/cell, whereas expression of 5×10^5 sites/cell produced maximal tyrosine phosphorylation of IRS-1. While the latter may reflect the limited abundance of IRS-1 in cells, the limiting step for the former remains unknown.

All developed clones retained similar sensitivity to E2, which strongly suggested that transfection of MCF-7 cells with the IGF-IR did not affect E2 receptor expression. Similar observations have been reported by other investigators who studied MCF-7 cells overexpressing the EGFR, IGF-IR, or c-erbB-2 [36, 38, 39].

In the next step, we tested monolayer growth of MCF-7/IGF-IR clones with special emphasis on their responsiveness to mitogenic effects of IGF-I and E2. We also examined cell growth under anchorage-independent conditions. Unexpectedly, in all MCF-7/IGF-IR clones, even those with the highest overexpression, the sensitivity to IGF-I was not significantly changed, and the responsiveness to this ligand was only moderately increased, compared with the corresponding parameters in MCF-7 cells. The cells with higher levels of IGF-IRs, however, exhibited increased responsiveness to low concentrations of IGF-I in the presence of E2. With higher concentrations of IGF-I, the synergistic effect of IGF-I and E2 was abolished, despite the fact that the cells retained normal E2 sensitivity. Consequently, in most MCF-7/IGF-IR clones, IGF-I alone, at a concentration of 4 ng/ml, produced the maximal mitogenic effect independent of E2. Our results are in agreement with the recent work of Daws *et al.* [36], who studied MCF-7 cells expressing approximately 2×10^5 IGF-IRs. In these cells, although the combined mitogenic effect of IGF-I and E2 was not increased, an enhanced response to low concentrations of IGF-I in the presence of E2 was noted. Interestingly, in MCF-7/IGF-IR cells, despite moderately increased responsiveness of DNA synthesis to IGF-I, the growth rate (increase of cell number) was not enhanced compared with MCF-7 cells.

These above observations suggest that in breast epithelial cells, the mitogenic effect mediated through the IGF-IR may be a saturated process. The exact nature of this phenomenon is not known. We speculate that in MCF-7/IGF-IR cells, the limited increase of response to IGF-I may be related to the translocation of a significant fraction of IGF-IRs to cell-cell boundaries

where they are not fully accessible for IGF-I stimulation (Fig. 6) (see below).

Under anchorage-independent conditions, partial loss of E2 requirements has been described in breast cancer cell lines overexpressing IGF-II [17] or IRS-1 [14]. In contrast, breast cancer cells overexpressing IGF-IRs generated by Daws *et al.* [36] as well as by our laboratory retained E2 requirement for growth in soft agar. It is possible that in both cases, the extent of receptor overexpression, or the abundance of available receptors, was not sufficient to override E2 dependence. It cannot be excluded, however, that in breast cancer cells, anchorage-independent growth requires activation of specific E2 signaling, which can be overridden by amplified IGF-II or IRS-1 signaling, but not IGF-IR signaling.

In the following part of this work, we assessed invasive properties of MCF-7/IGF-IR cells *in vitro* as well as the effects of IGF-IR overexpression on cell-cell adhesion. MCF-7 cells are poorly invasive [25] but their invasive properties *in vitro* can be enhanced, for instance, by the overexpression of H-ras [37-40]. We demonstrated that overexpression of the IGF-IR did not stimulate invasiveness of MCF-7 cells. In contrast, we observed that high levels of IGF-IRs actually promoted cell-cell adhesion and formation of large organoid-like structures on Matrigel (Fig. 4). Importantly, in this assay, the extent of aggregation (number and sizes of aggregates) paralleled the level of IGF-IRs. Moreover, the cells expressing more than 1×10^6 sites/cell not only survived in the aggregates for the longest period but also continued to multiply within the formed clusters. This suggested that the IGF-IR, by stimulating cell-cell adhesion, promoted proliferation of aggregated cells and protected cells from death.

The role of the IGF-IR in cell-cell adhesion was further substantiated by the evidence that IGF-I stimulated the aggregation of MCF-7 and MCF-7/IGF-IR cells (Fig. 5B). The aggregation of these cells was blocked in the presence of anti-E-cadherin antibody, which demonstrated that IGF-IR-enhanced adhesion requires functional E-cadherin (Fig. 5B). Our findings are consistent with the data of Bracke *et al.* [26], who demonstrated that in the invasive breast cancer cell line MCF-7/6, IGF-I stimulated cell aggregation in the absence but not in the presence of an anti-E-cadherin antibody.

The direct visualization by immunofluorescence microscopy revealed that in MCF-7/IGF-IR cells, the IGF-IR co-localizes with E-cadherin at the points of cell-cell contacts (Fig. 6). To our knowledge, this is the first demonstration of co-localization of the IGF-IR with a cell-cell adhesion molecule. The interaction of the IGF-IR with the E-cadherin complex was also confirmed by Western immunoblotting. Specifically, we found that in MCF-7 cells and MCF-7/IGF-IR clones, E-cadherin

associated with IRS-1, SHC, and the IGF-IR. In MCF-7/IGF-IR cells, more IGF-IR appeared to be contained within E-cadherin complexes (Fig. 7). Interestingly, tyrosine phosphorylation of E-cadherin-associated SHC and IGF-IRs was not evidently increased in cells exposed to IGF-I for 48 h, whereas tyrosine phosphorylation of IRS-1 in the E-cadherin complex was quite prominent (Fig. 7). The molecular bases of this effect remain to be determined. It is possible that incorporation of the IGF-IR and SHC into adhesion complex accelerates dephosphorylation. IRS-1, resistant to this dephosphorylation, is probably a substrate of a different phosphatase(s).

In several experiments, we consistently observed an inhibitory effect of IGF-I on tyrosine phosphorylation of a 120-kDa protein whose position corresponded to that of E-cadherin (Fig. 7, MCF-7 cells, clone 12 and clone 15). Possibly, one of the functions of the IGF-IR in MCF-7 cells is to increase cell aggregation through dephosphorylation of E-cadherin. The interplay between growth factor- or oncoprotein-induced signaling and the regulation of cell-cell adhesion has already been described. For instance, EGF interferes with phosphorylation status of molecules engaged in adherens-type junctions, i.e., β -catenin is phosphorylated upon EGF stimulation [41]. In addition, expression of v-src causes tyrosine phosphorylation of E-cadherin and disrupts the cadherin-catenin complexes [42]. Cell-cell association can also be regulated by modification of the expression of adhesion proteins. For instance, overexpression of the ERB-B2 receptor or treatment with TGF- β inhibited expression of E-cadherin in normal mammary cells [43, 44]. In our model, there was no apparent modulation of E-cadherin expression.

Our experiments are still insufficient to resolve whether E-cadherin binds directly to either the IGF-IR or one of its substrates or if other intermediate proteins may be necessary to mediate this association. In fact, our preliminary data demonstrated that the IGF-IR is also present in β - and α -catenin precipitates. Similarly, since both IRS-1 and SHC can associate with the IGF-IR, binding of only one of those proteins to E-cadherin should be sufficient to form a multielement complex. Regardless of the nature of the association, the evident proximity of cell-cell adhesion molecules and the elements of IGF-IR signaling support our data implicating the IGF-IR in the regulation of epithelial aggregation.

The mechanism of IGF-IR-dependent cell-cell adhesion is currently unknown. The hypothesis that catalytic function of the receptor is involved is supported by the notion that in the presence of IGF-I, aggregation was induced and partial dephosphorylation of E-cadherin was observed. The other possibility is that the clusterization of receptors, due to activation by IGF-I or resulting from overexpression, induced concomitant

clusterization of associated E-cadherin complexes, which created stronger contacts and promoted aggregation.

In summary, our findings suggest a complex role of the IGF-IR in breast cancer. On one hand, increased levels of IGF-IRs induce hypersensitivity to IGF-I in the presence of E2, which may provide a growth advantage for cancer cells under conditions of low IGF-I availability (for example, in patients undergoing tamoxifen treatment [45]). On the other hand, the overexpression of the IGF-IR inhibits cell scattering, and, therefore, may have a role in the growth of noninvasive, differentiated breast tumors. The latter supports the data demonstrating that in breast cancer, higher levels of receptor predict better prognosis [11]. The "antiscattering" function of the IGF-IR, however, does not seem to be universal. In other systems (such as invasive lung carcinoma), this receptor is required for metastatic activity [46]. Unquestionably, more studies are required to define the role of IGF signaling in metastasis as well as in other neoplastic processes.

We are grateful to Drs. Renato Baserga, Gerald Grunwald, and Jerzy W. Kolaczynski for critically reading the manuscript and to David Dicker for his expert assistance with FACS analysis. This work was supported in part by NIH Grant DK48969 (E.S.). E.S. is a recipient of a Career Development Award TR950198 from the U.S. Army.

REFERENCES

1. Ullrich, A., Gray, A., Tam, A. W., Yang-Feng, T., Tsubokawa, M., Collins, C., Henzel, W., Le Bon, T., Kahuria, S., Chen, E., Jakobs, S., Francke, U., Ramachandran, J., and Fujita-Yamaguchi, Y. (1986) *EMBO J.* **5**, 2503-2512.
2. Myers, M. G., Sun, X. J., and White, M. F. (1994) *Trends Biochem. Sci.* **19**, 289-293.
3. Keller, S. R., and Lienhard, G. E. (1994) *Trends Cell Biol.* **4**, 115-119.
4. Giorgetti, S., Pelicci, P. G., Pelicci, G., and Van Obberghen, E. (1994) *Eur. J. Biochem.* **223**, 195-202.
5. Pelicci, G., Lanfrancone, L., Grignani, F., McGlade, J., Cavallo, F., Forni, G., Nicoletti, I., Grignani, F., Pawson, T., and Pelicci, P. G. (1992) *Cell* **70**, 93-104.
6. Vuori, K., and Ruoslahti, E. (1994) *Science* **266**, 1576-1578.
7. Spargaren, M., Bischoff, J. R., and McCormick, F. (1995) *Gene Expr.* **4**, 345-346.
8. Joneson, T., White, M. A., Wigler, M. H., and Bar-Sagi, D. (1996) *Science* **271**, 810-812.
9. Rubin, R., and Baserga, R. (1995) *Lab. Invest.* **73**, 311-331.
10. Ellis, M. J. C., Singer, C., Hornby, A., Rasmussen, A., and Cullen, K. J. (1994) *Breast Cancer Res. Treat.* **31**, 249-261.
11. Papa, V., Gliozzo, B., Clark, G. M., McGuire, W. L., Moore, D., Fujita-Yamaguchi, Y., Vigneri, R., Goldfine, I. D., and Pezzino, V. (1993) *Cancer Res.* **53**, 3735-3740.
12. Rocha, R. L., Hilsenbeck, S. G., Jackson, J. G., and Yee, D. (1995) *Breast Cancer Res. Treat. Suppl.* **37**, 55.
13. Stewart, A. J., Johnson, M. D., May, F. E. B., and Westley, B. R. (1990) *J. Biol. Chem.* **265**, 21172-21178.

14. Surmacz, E., and Burgaud, J.-L. (1995) *Clin. Cancer Res.* **1**, 1429–1436.
15. Dickson, R. B., and Lippman, M. E. (1987) *Endocr. Rev.* **8**, 29–43.
16. Figueroa, J. A., and Yee, D. (1992) *Breast Cancer Res. Treat.* **22**, 81–90.
17. Cullen, K. J., Lippman, M. E., Chow, D., Hill, S., Rosen, N., and Zwiebel, J. A. (1992) *Mol. Endocrinol.* **6**, 91–100.
18. Arteaga, C. L., and Osborne, C. K. (1989) *Cancer Res.* **49**, 6237–6241.
19. Yee, D., Jackson, J. G., Kozelsky, T. W., and Figueroa, J. A. (1994) *Cell Growth Differ.* **5**, 73–77.
20. Neuenschwander, S., Roberts, C. T., Jr., and LeRoith, D. (1995) *Endocrinology* **136**, 4298–42303.
21. Guerra, F. K., Eijan, A. M., Puricelli, L., Alonso, D. E., Joffe, E. B. D., Kornblihtt, A. R., Charreau, E. H., and Elizalde, P. V. (1996) *Int. J. Cancer* **65**, 812–820.
22. Pantel, K., Schlimok, G., Angstwurm, M., Passlick, B., Izbicki, J. R., Johnson, J. P., and Riethmuller, G. (1995) in *Cell Adhesion and Human Disease*, Ciba Foundation Symposium 189, pp. 157–173, Wiley, Chichester.
23. Birchmeier, W., Hulsken, J., and Behrens, J. (1995) in *Cell Adhesion and Human Disease*, Ciba Foundation Symposium 189, pp. 124–141, Wiley, Chichester.
24. Birchmeier, W., Hulsken, J., and Behrens, J. (1995) *Cancer Surveys* **24**, 129–140.
25. Sommers, C., Gelmann, E. P., Kemler, R., Cowin, P., and Byers, S. W. (1994) *Cancer Res.* **54**, 3544–3552.
26. Bracke, M. E., Vyncke, B. M., Bruyneel, E. A., Vermeulen, S. J., De Bruyne, G. K., Van Larebeke, N. A., Vleminckx, K., Van Roy, F. M., and Mareel, M. M. (1993) *Br. J. Cancer* **68**, 282–289.
27. Bae, S.-N., Arand, G., Azzam, H., Pavasant, P., Torri, J., Frandsen, T. L., and Thompson, E. W. (1993) *Breast Cancer Res. Treat.* **24**, 241–255.
28. Vleminckx, K., Vakaet, L., Jr., Mareel, M., Fiers, W., and Van Roy, F. (1991) *Cell* **66**, 107–119.
29. Bracke, M. E., Charlier, C., Bruyneel, E. A., Labit, C., Mareel, M. M., and Castronovo, V. (1994) *Cancer Res.* **54**, 4607–4609.
30. Miura, M., Surmacz, E., Burgaud, J.-L., and Baserga, R. (1995) *J. Biol. Chem.* **270**, 22639–22644.
31. Soos, M. A., Whittaker, J., Lammers, R., Ullrich, A., and Siddle, K. (1990) *Biochem. J.* **270**, 383–390.
32. Zhou-Li, F., D'Ambrosio, C., Li, S., Surmacz, E., and Baserga, R. (1995) *Mol. Cell. Biol.* **15**, 4232–4239.
33. Goldstein, A., Arronow, L., and Kalman, S. M. (1974) in *Principles of Drug Action: The Basis of Pharmacology*, pp. 82–111, Wiley, Chichester.
34. Li, S., Ferber, A., Miura, M., and Baserga, R. (1994) *J. Biol. Chem.* **269**, 32558–32564.
35. Pietrkowski, Z., Lammers, R., Carpenter, G., Soderquist, A., Limardo, M., Phillips, P., Ullrich, A., and Baserga, R. (1992) *Cell Growth Differ.* **3**, 199–205.
36. Daws, M. R., Westley, B. R., and May, F. E. B. (1996) *Endocrinology* **137**, 1177–1186.
37. Kleinman, D., Karas, M., Roberts, C. T., Jr., LeRoith, D., Philip, M., Sagev, Y., Levy, J., and Sharoni, Y. (1995) *Endocrinology* **136**, 2531–2537.
38. Miller, D. L., El-Ashry, D., Cheville, A. L., Liu, Y., McLeskey, S. W., and Kern, F. (1994) *Cell Growth Differ.* **5**, 1263–1274.
39. Liu, Y., El-Ashry, D., Chen, D., Yi Fan Ding, I., and Kern, F. G. (1995) *Breast Cancer Res. Treat.* **34**, 97–117.
40. Gelmann, E. P., Thompson, E. W., and Sommers, C. (1992) *Int. J. Cancer* **50**, 665–669.
41. Hoschuetzky, H., Aberle, H., and Kemler, R. (1994) *J. Cell Biol.* **127**, 1375–1380.
42. Behrens, J., Vakaet, L., Friis, R., Winterhager, E., Van Roy, F., Mareel, M. M., and Birchmeier, W. (1993) *J. Cell Biol.* **120**, 757–766.
43. D'Souza, B., and Taylor-Papadimitriou, J. (1994) *Proc. Natl. Acad. Sci. USA* **91**, 7202–7204.
44. Miettinen, P. J., Ebner, R., Lopez, A. R., and Derynck, R. (1994) *J. Cell Biol.* **127**, 2022–2036.
45. Colletti, R. B., Roberts, J. D., Devlin, J. T., and Copeland, K. C. (1989) *Cancer Res.* **49**, 1882–1884.
46. Long, L., Rubin, R., Baserga, R., and Brodt, P. (1995) *Cancer Res.* **55**, 1006–1009.

Received September 11, 1996

Revised version received November 25, 1996

Tamoxifen Interferes with the Insulin-like Growth Factor I Receptor (IGF-IR) Signaling Pathway in Breast Cancer Cells¹

Marina A. Guvakova and Ewa Surmacz²

Kimmel Cancer Institute, Thomas Jefferson University, Philadelphia, Pennsylvania 19107

Abstract

The insulin-like growth factor I receptor (IGF-IR) is involved in the control of breast cancer cell growth. The cytostatic activity of tamoxifen (Tam), a nonsteroidal antiestrogen, is partially mediated through interference with IGF-I-R-dependent proliferation, yet the effects of Tam on IGF-IR intracellular signaling have never been elucidated. Consequently, we investigated how Tam modifies the IGF-IR signaling pathway in estrogen receptor-positive MCF-7 breast cancer cells and in MCF-7-derived clones overexpressing either the IGF-IR (MCF-7/IGF-IR cells) or its major substrate, IRS-1 (MCF-7/IRS-1 cells). MCF-7/IGF-IR and MCF-7/IRS-1 cells exhibit greatly reduced estrogen growth requirements but retain estrogen receptors and express sensitivity to antiestrogens comparable to that in the parental cells. In all tested cell lines, regardless of the amplification of IGF signaling, a 4-day treatment with 10 nM Tam produced a similar cytostatic effect. In MCF-7 and MCF-7/IGF-IR cells, growth inhibition by Tam was associated with the reduced tyrosine phosphorylation of the IGF-IR in the presence of IGF-I; however, the basal level of the IGF-IR remained unaffected. Moreover, Tam inhibited both basal and IGF-I-induced tyrosine phosphorylation of IRS-1, which was accompanied by down-regulation of IRS-1-associated phosphatidylinositol 3'-kinase activity and reduced IRS-1/growth factor receptor-bound protein 2 (GRB2) binding. In contrast, under the same treatment, tyrosine phosphorylation of Src-homology/collagen proteins (SHC; another substrate of the IGF-IR) and SHC/GRB2 binding were elevated. The protein levels of the IGF-IR and IRS-1 were not modified by Tam, whereas SHC protein expression was either not affected or moderately decreased by the treatment.

In summary, this work provides the first evidence that in MCF-7 cells, cytostatic effects of Tam are associated with the modulation of IGF-IR signaling, specifically with: (a) down-regulation of IGF-I-induced tyrosine phosphorylation of the IGF-IR; (b) inhibition of IRS-1/phosphatidylinositol 3'-kinase signaling; and (c) up-regulation of SHC tyrosine phosphorylation and increased SHC/GRB2 binding. It is hypothesized that dephosphorylation of IRS-1 could be a major contributing factor in Tam cytostatic activity.

Introduction

The activation of the IGF-IR,³ through a paracrine, autocrine, or endocrine mechanism, appears to play a critical role in the regulation of breast cancer cell growth (1). The IGF-IR levels are significantly

higher in breast cancer than in normal breast tissue or benign tumors (1-3). The IGFs are potent mitogens for cultured breast cancer cells, and their expression has been documented in the epithelial and/or stromal component of breast tumors (1). In primary breast cancer, a correlation has been found between tumor size, the levels of IRS-1 (a cellular substrate of the IGF-IR), and recurrence of the disease (4). In MCF-7 breast cancer cells, the overexpression of either IRS-1 (5), the IGF-IR (6), or IGF-II (7) have been shown to reduce estrogen growth dependence. On the other hand, it has been demonstrated that blockade of IGF-IR signaling with, for instance, anti-IGF-IR antibodies (1), antisense RNA to the IGF-IR (8), and antisense oligodeoxynucleotides to IRS-1 (5) restricts breast cancer cell growth *in vitro* or *in vivo*.

The activation of the IGF-IR tyrosine kinase results in the stimulation of diverse intracellular pathways involving different signaling substrates (9). The best characterized substrates of the IGF-IR are IRS-1 and SHC. IRS-1 is a docking protein that, upon tyrosine phosphorylation by the IGF-IR, recruits several effector proteins through SH2-type interactions. For instance, IRS-1 binds and activates PI-3 kinase and SH2 phosphatase as well as stimulates Ras/MAP pathway through the binding of GRB-2/SOS complexes (9). Moreover, IRS-1 has been found to interconnect with JAK-STAT (10) and integrin signaling pathways (11). SHC proteins are substrates of most tyrosine kinase receptors, many nonreceptor kinases and certain phosphatases (12, 13). Tyrosine phosphorylated SHC, similar to IRS-1, may activate Ras/MAP signaling cascade through the GRB2/SOS complex (12).

Tam, a nonsteroidal antiestrogen with partial agonist activity, is commonly used in adjuvant therapy in breast cancer management (14). Tam inhibits ER-dependent growth but also interferes with polypeptide growth factor signaling (14). The known effects of Tam or its derivative 4-OH-Tam on the IGF system in breast cancer cells include: inhibition of IGF-I stimulated growth (14, 15), modulation of IGFBP expression (1), reduced secretion of autocrine IGF (16), down-regulation of plasma levels of IGF-I in breast cancer patients (17), and decreased levels of IGF-I binding sites (18, 19). The interaction of Tam with the IGF-IR signaling pathway has not been characterized, partly because of the lack of adequate cellular models. Here, we investigated this aspect of Tam action using ER-positive MCF-7 cells as well as different MCF-7-derived cell lines overexpressing the elements of IGF-IR signaling.

Materials and Methods

Cell Lines and Cell Culture Conditions. MCF-7 cells were routinely grown in DMEM:F12 (1:1) containing 5% calf serum (6). In the experiments requiring estrogen-free conditions, the cells were cultured in phenol red-free DMEM containing 0.5 mg/ml BSA, 1 μ M FeSO₄ and 2 mM L-glutamine (PRF-SFM; Ref. 6).

MCF-7/IGF-IR, clones 12 and 15, and MCF-7/IRS-1, clone 3 were developed by stable transfection with the expression vectors pcDNA3/IGF-IR and CMV-IRS-1, respectively, and were characterized in detail previously (5, 6). The clones were maintained in culture for a maximum of 3 months in growth medium supplemented with 200 μ g/ml G418.

Received 3/7/97; accepted 5/13/97.

The costs of publication of this article were defrayed in part by the payment of page charges. This article must therefore be hereby marked *advertisement* in accordance with 18 U.S.C. Section 1734 solely to indicate this fact.

¹ This work was supported in part by Grant DK 48969 from the NIH (to E. S.). E. S. is a recipient of Career Development Award DAMD 17-96-1-6250 from the Department of the Army.

² To whom requests for reprints should be addressed, at Kimmel Cancer Institute BLSB 606A, Thomas Jefferson University, 233 South 10th Street, Philadelphia, PA 19107. Phone: (215) 503-4512; Fax: (215) 923-0249.

³ The abbreviations used are: IGF-IR, insulin-like growth factor I receptor; ER, estrogen receptor; GRB2, growth factor receptor-bound protein 2; IGFBP, IGF binding protein; IRS-1, insulin receptor substrate 1; MCF-7/IGF-IR, MCF-7 cells overexpressing IGF-IRs; MCF-7/IRS-1, MCF-7 cells overexpressing IRS-1; PI-3 kinase, phosphatidylinositol 3'-kinase; PRF-SFM, phenol red-free serum-free medium; SH2, src homology 2 domain; Tam, tamoxifen; SHC, Src-homology/collagen proteins; MAP, mitogen-activated protein kinase.

Cell Growth Assay. Cells (1×10^5) were plated in 24-well plates in DMEM:F12 (1:1) containing 5% calf serum. The next day, designed as day 0 of the experiment, the cells were shifted to either PRF-SFM or PRF-SFM supplemented with 0.1–100 nM Tam. For each cell line, the number of cells at day 0 was taken as 100% (control). The relative increase (percentage over control) in cell number was determined after 4 days of Tam treatment.

Western Blotting and Immunoprecipitation. The levels of the IGF-IR, IRS-1, SHC, as well as tyrosine phosphorylation of these proteins, were measured by Western blotting. The protein lysates (250–500 μ g) were obtained as described previously (6) and immunoprecipitated with the following antibodies: for IGF-IR, anti-IGF-IR monoclonal antibody alpha-IR3 (Oncogene Science); for IRS-1, anti-IRS-1 polyclonal antibody (UBI); and for SHC, anti-SHC polyclonal antibody (Transduction Laboratories). The immunoprecipitates were resolved by PAGE, and the IGF-IR, IRS-1, or SHC proteins were immunodetected with the following antibodies: for IRS-1, anti-IRS-1 polyclonal antibody (UBI); for IGF-IR and its M_r 200,000 precursor (20), anti-IGF-IR polyclonal antibody (Santa Cruz); and for SHC, anti-SHC monoclonal antibody (Transduction Laboratories). Tyrosine phosphorylation of the above proteins was detected by immunoblotting with an anti-phosphotyrosine monoclonal antibody PY20 (Transduction Laboratories). The intensity of bands was assessed by laser densitometry scanning.

PI-3 Kinase Activity. The activity of PI-3 kinase associated with IRS-1 was assessed by standard protocol provided by the manufacturer of the IRS-1 antibody (UBI). In brief, 500 μ g of protein lysate were immunoprecipitated with an anti-IRS-1 polyclonal antibody. The IRS-1 immunoprecipitates were incubated *in vitro* in the presence of 200 μ g/ml phosphatidylinositol (Sigma Chemical Co.) and 10 μ Ci [γ - 32 P]ATP for 30 min. The products of the kinase reaction were resolved on TLC plates (Eastman Kodak), and the spots corresponding to PI-3 phosphates were identified by autoradiography. The spots were then cut from the plates, and their radioactivity was counted with a beta counter. For each cell line, PI-3 kinase activity obtained in SFM was taken as 100% (control).

Results

Tam Inhibits the Growth of MCF-7 Breast Cancer Cells Overexpressing Either the IGF-IR or IRS-1. We studied whether Tam is able to inhibit the growth of MCF-7 cells with amplified IGF-IR signaling (MCF-7/IGF-IR and MCF-7/IRS-1 cells). The estrogen growth requirements in these cells are abolished or significantly reduced; however, the cells retain expression of the ER (5, 6). The effect of Tam on growth was studied in MCF-7/IGF-IR, clone 12 (expressing 5×10^5 IGF-I binding sites/cells; 8-fold IGF-IR overexpression over the levels in MCF-7 cells), MCF-7/IGF-IR, clone 15

(3×10^6 sites/cells; 50-fold IGF-IR overexpression), and in MCF-7/IRS-1, clone 3 (a 9-fold overexpression of IRS-1 over that in MCF-7 cells); MCF-7 cells were used as a control. The cells were cultured in PRF-SFM for 4 days in the presence of different concentrations of Tam (0.1–100 nM). Tam treatment suppressed growth of all cell lines in a dose-dependent manner (Fig. 1). Specifically, in all cells, 0.1, 1.0, and 10 nM Tam reduced proliferation by at least 12, 34, and 50%, respectively. The extent of Tam-induced growth inhibition in cells cultured for 4 days in PRF-SFM with 20 ng/ml IGF-I was comparable (data not shown). Treatment with 100 nM Tam was always cytotoxic. Consequently, Tam at a concentration of 10 nM was used in all further experiments.

Tam Interferes with IGF-I-induced Tyrosine Phosphorylation of the IGF-IR in MCF-7/IGF-IR Cells. To investigate the effects of Tam on IGF-IR signaling, we assessed tyrosine phosphorylation and protein levels of the IGF-IR in MCF-7 and MCF-7/IGF-IR, clone 15 cells. In cells cultured in PRF-SFM plus IGF-I, the IGF-IR tyrosine phosphorylation was always elevated compared with that in PRF-SFM (Fig. 2). After 4 days of treatment, the effects of Tam on the basal level of IGF-IR tyrosine phosphorylation were minimal (Fig. 2A); specifically, in several experiments either no modification or slight (\sim 15%) up- or down-regulation were noticeable. However, Tam reduced IGF-I-induced tyrosine phosphorylation by 60% in MCF-7 cells and by 30% in MCF-7/IGF-IR cells (Fig. 2B).

The IGF-IR protein levels were not significantly modulated by Tam, as determined by laser densitometry scanning (Fig. 2). Similarly, the levels of the IGF-IR precursor were not affected by the treatment (Fig. 2A).

Inhibition of Cell Growth by Tamoxifen Is Associated with Dephosphorylation of IRS-1. In all tested cell lines, but especially in the clones with amplified IGF-IR signaling (MCF-7/IGF-IR, clones 12 and 15, and in MCF-7/IRS-1 cells), a basal level of IRS-1 tyrosine phosphorylation was evident even after prolonged culture in PRF-SFM, which reflected cellular response to autocrine IGFs, as shown previously (Refs. 5 and 6; Fig. 3, A and B). The addition of 10 nM Tam to PRF-SFM produced a cytostatic effect (Fig. 1), which was accompanied by a marked dephosphorylation of IRS-1 on tyrosine residues in the cells studied. Specifically, the basal level of IRS-1 tyrosine phosphorylation was reduced by 29, 35, and 48% in MCF-7/IGF-IR, clone 12, MCF-7/IGF-IR, clone 15, and MCF-7/IRS-1 cells, respectively (Fig. 3A). In MCF-7 cells, due to a low basal level of IRS-1

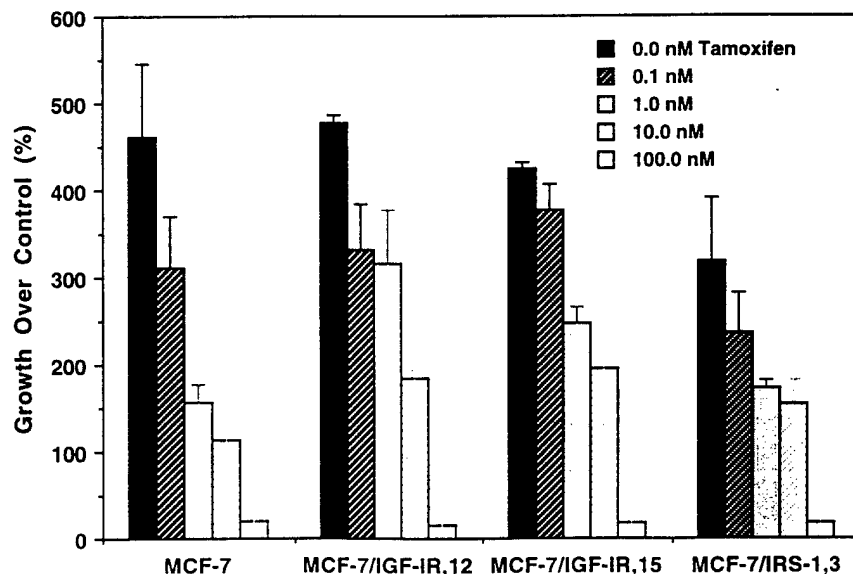


Fig. 1. Tam inhibits the growth of MCF-7 cells overexpressing either the IGF-IR or IRS-1. The cells were treated as described in "Materials and Methods." The results represent the percentage of growth inhibition relative to control (100%) in PRF-SFM. The results are means from at least four experiments. Bars, SE.

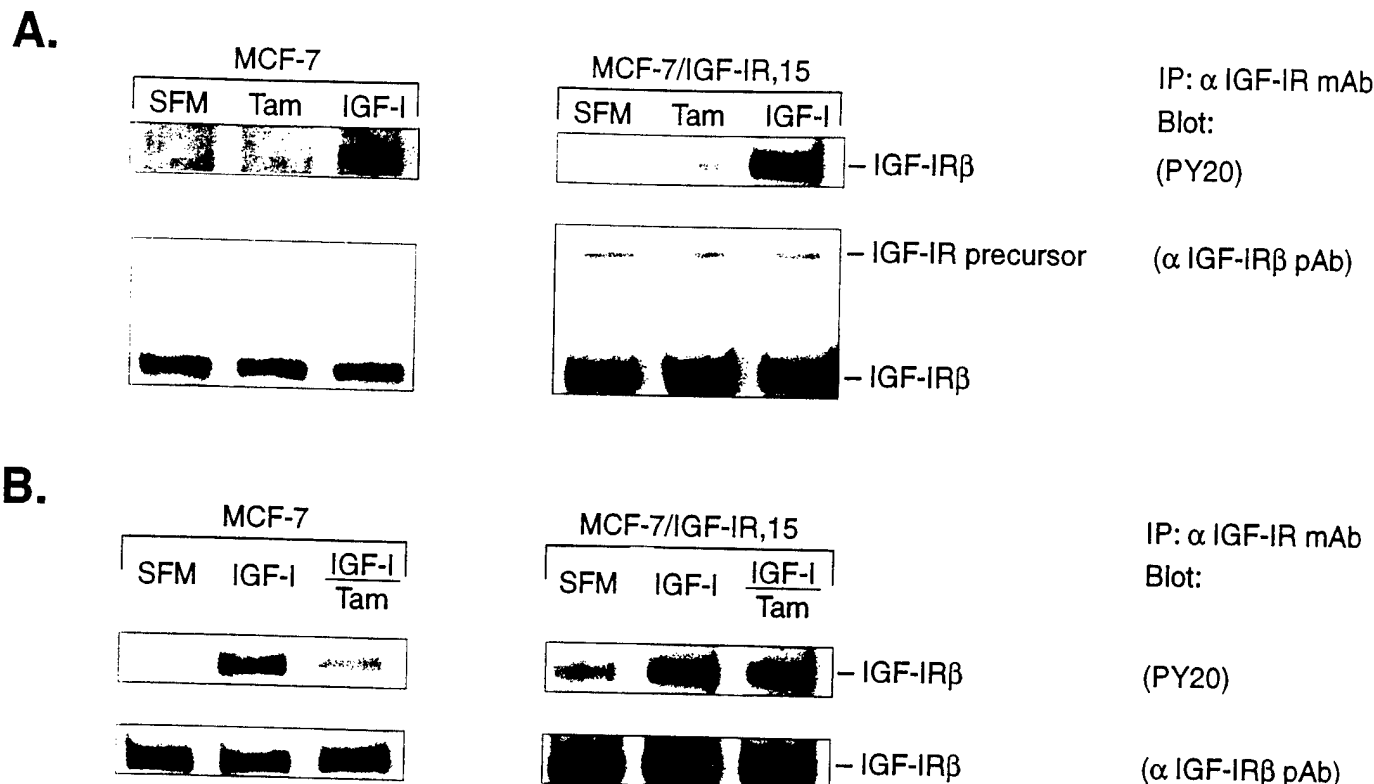


Fig. 2. Effects of Tam on the IGF-IR. **A.** Tam effect on basal level of IGF-IR tyrosine phosphorylation. The cells were lysed after 3 days of incubation in either PRF-SFM (SFM), PRF-SFM plus 10 nM Tam (Tam), or PRF-SFM plus 50 ng/ml IGF-I (IGF-I). Tyrosine phosphorylation and protein level of the IGF-IR were determined after immunoprecipitation of 500 μ g of protein lysates with an anti-IGF-IR monoclonal antibody followed by Western blotting with the indicated antibodies. **B.** Tam blocks IGF-I-induced tyrosine phosphorylation of the IGF-IR. Lane IGF-I/Tam, cells were cultured in PRF-SFM with 50 ng/ml IGF-I and 10 nM Tam; other conditions were as described for A. Representative results from four experiments are shown.

phosphorylation, the effect of Tam was not measurable. The interference of Tam with IRS-1 signaling was further studied in MCF-7/IRS-1 cells (Fig. 3B). The IGF-I-stimulated and basal levels of IRS-1 phosphorylation were suppressed in the presence of the drug by approximately 43% (Fig. 3B). The dephosphorylation of IRS-1 was accompanied by its dissociation from both p85 subunit of PI-3 kinase and GRB2 (Fig. 3B). Similar effects of Tam on IRS-1 tyrosine phosphorylation (approximately 27% inhibition) were seen in MCF-7/IGF-IR, clone 15 cells (data not shown).

In addition, Tam suppressed the activity of IRS-1-associated PI-3 kinase in cells stimulated with IGF-I; the inhibition by 43, 92, and 128% was seen in MCF-7, MCF-7/IGF-IR, and MCF-7/IRS-1, respectively (Fig. 3C). The effects of Tam on PI-3 kinase in cells cultured in PRF-SFM were not measurable.

In several repeat experiments, IRS-1 protein levels were not affected by long-term treatment with Tam (Fig. 3, A and B).

Tamoxifen Increases Tyrosine Phosphorylation of SHC. Of note, in all studied cell lines the cytostatic action of Tam was associated with the elevated tyrosine phosphorylation of p52^{SHC} and p46^{SHC} (Fig. 4). The activation of p52^{SHC} was especially prominent; specifically, compared with SHC status in untreated cells, a 34, 110, and 100% augmentation of p52^{SHC} tyrosine phosphorylation was observed in MCF-7, MCF-7/IGF-IR, and MCF-7/IRS-1 cells, respectively. Moreover, the hyperphosphorylation of p52^{SHC} was followed by an its increased binding to GRB2 (Fig. 4).

In contrast, in all cell lines, a 4-day exposure to IGF-I decreased tyrosine phosphorylation of p52^{SHC} by approximately 40% compared with that in PRF-SFM and induced dissociation of SHC/GRB2 complexes (Fig. 4).

Tam treatment produced a consistent down-regulation of p52^{SHC} and p46^{SHC} levels by approximately 35% in MCF-7/IGF-IR, clone 15

and MCF-7/IRS-1 cells but not in MCF-7 cells (Fig. 4). In contrast, SHC protein expression was not modulated by IGF-I (Fig. 4).

Effect of Tamoxifen on ERK2. Because IRS-1 and SHC, via GRB2/SOS, may activate Ras/MAP signaling pathway, we assessed MAP (ERK2) kinase activity in cells exposed to Tam or cultured for 4 days in PRF-SFM in the presence or absence of exogenous IGF-I. We found no differences in ERK2 activity under these conditions, measured in an *in vitro* assay, using myelin basic protein as a substrate (data not shown).

Discussion

Experimental evidence suggests an important role of the IGF-R in the pathobiology of breast tumors (1–3). Activation of the IGF-IR promotes proliferation and transformation as well as cell-cell and cell-substrate interactions in breast cancer cells (1, 5, 6, 21). Conversely, the blockade of IGF signaling results in the inhibition of breast cancer growth (1, 5, 8). Tam, or its derivative 4-OH-Tam, have been shown to inhibit IGF-IR-dependent growth through different mechanisms, such as down-regulation of autocrine IGF secretion (16) or modulation of IGF-BPs expression (1). In addition, in MCF-7 breast cancer cells, Tam and 4-OH-Tam decreased expression of IGF-I binding sites by approximately 30% (19) and 60% (18), respectively.

The effects of Tam on the IGF signal transduction pathway are unknown. Here, we report for the first time the modulation of the IGF-IR intracellular signaling pathways associated with the cytostatic action of Tam. Our studies focused on tyrosine kinase activity and protein levels of the IGF-IR and its two major cellular substrates, IRS-1 and SHC. Preliminary data from Rocha *et al.* (4) documented that IRS-1 is expressed in primary breast tumors and its levels correlate with increased recurrence. The status of SHC and its relation with

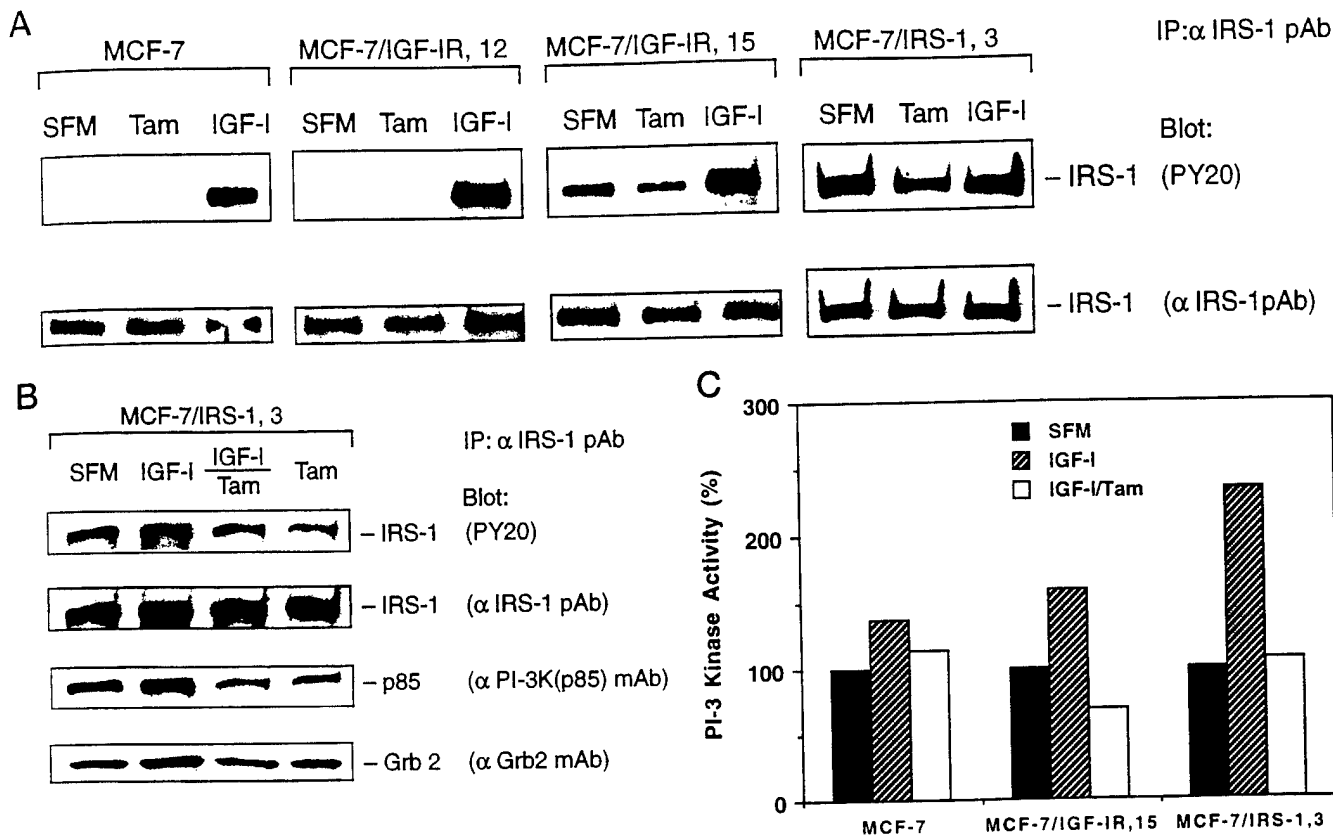


Fig. 3. Effects of Tam on IRS-1-mediated signaling. **A**, effects of Tam on IRS-1 tyrosine phosphorylation. MCF-7 cells, MCF-7/IGF-IR, clones 12 and 15, and MCF-7/IRS-1, clone 3, were incubated in PRF-SFM (SFM), PRF-SFM plus 10 nM Tam (Tam), or PRF-SFM plus 50 ng/ml IGF-I (IGF-I) for 3 days. IRS-1 was immunoprecipitated from 300 μ g of protein lysates, and tyrosine phosphorylation levels were detected with PY-20 antibody. IRS-1 protein level was determined in the original blot, after stripping and reprobing with an anti-IRS-1 antibody. Representative results from five experiments are shown. **B**, effects of Tam on IRS-1 signaling in MCF-7/IRS-1 cells. MCF-7/IRS-1, clone 3, was cultured for 4 days in either PRF-SFM (SFM), PRF-SFM plus 50 ng/ml IGF-I alone (IGF-I), PRF-SFM plus 50 ng/ml IGF-I with 10 nM Tam (IGF-I/Tam), or PRF-SFM plus 10 nM Tam (Tam). IRS-1 was immunoprecipitated from 250 μ g of lysates, and IRS-1 protein level and tyrosine phosphorylation were detected as described above. Amounts of p85 of PI-3 kinase and GRB2 associated with IRS were determined in original nitrocellulose filters after stripping and reprobing with specific antibodies. **C**, Tam effects on IRS-1 associated PI-3 kinase activity. The cells were incubated in PRF-SFM (SFM), PRF-SFM plus 50 ng/ml IGF-I (IGF-I), or PRF-SFM plus 50 ng/ml IGF-I and 10 nM Tam (IGF-I/Tam) for 3 days. IRS-1 was precipitated from 500 μ g of cell lysates from each cell line. The activity of PI-3 kinase associated with IRS-1 was assessed *in vitro* as described in "Materials and Methods." The results are expressed as percentage of increase over control levels in SFM (100%). Representative data are shown.

different prognostic markers is not known. Our experiments with MCF-7 cells expressing antisense RNA to either IRS-1 or SHC demonstrated that normal levels of both substrates are critical in sustaining monolayer and anchorage-independent growth.⁴ In addition, IRS-1 signaling appears to play a role in the protection from apoptosis *in vitro*.⁴

Here, we looked at the status of IRS-1 and SHC in the state of growth inhibition induced by Tam. We approached this problem using MCF-7 cells as well as more sensitive cellular models, *i.e.*, MCF-7-derived clones overexpressing either the IGF-IR or IRS-1 (5, 6). The amplification of IGF-IR signaling in MCF-7 cells promotes growth responsiveness to IGF-I and abrogates estrogen growth requirements but does not influence ER expression and function (5, 6). In this work, we demonstrated that estrogen independence in MCF-7/IGF-IR and MCF-7/IRS-1 cells does not circumvent sensitivity to cytostatic action of Tam. Remarkably, the inhibition of growth was similar in all studied cell lines, regardless of the amplification of IGF-IR signaling. With this experimental system we have made several important observations:

(a) Tam had no apparent effect on IGF-IR protein levels or the levels of its precursor, at least in a 4-day experiment. Other studies

demonstrated a small (30%) down-regulation of IGF binding sites in Tam-treated MCF-7 cells (19); however, binding assays were performed without discriminating IGF-I association with membrane IGF-BPs, which could result in miscalculation of IGF-IR levels (22).

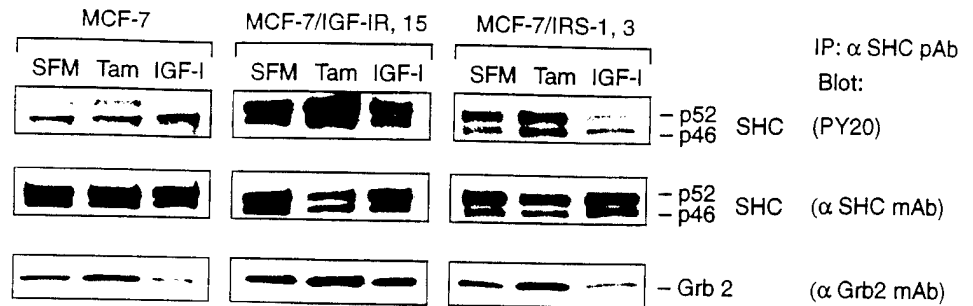
(b) Tam inhibited IGF-I-induced tyrosine phosphorylation of the IGF-IR. It is unlikely that this effect was mediated exclusively through the reduction of the amount of autocrine IGFs because Tam effectively suppressed autocrine growth without modification of the basal IGF-IR tyrosine phosphorylation (in PRF-SFM; Figs. 1 and 2). Why the effect of Tam on IGF-IR activation is evident in the presence of excess IGF-I but not with autocrine IGFs remains to be clarified: possibly, the regulation of the phosphatase system is different under these two conditions. This observation, however, suggests that continuing dephosphorylation of the IGF-IR is not critical for Tam-induced growth arrest.

(c) Tam treatment resulted in the persisting dephosphorylation of IRS-1 on tyrosine residues, apparently in the presence of both autocrine and exogenous IGF-I. The attenuation of IRS-1 tyrosine phosphorylation by Tam was accompanied by down-regulation of IRS-1-associated PI-3 kinase activity and dissociation of GRB2 from IRS-1. Our findings agree with preliminary data of Kleinman *et al.* (23), who demonstrated that Tam inhibited tyrosine phosphorylation of a M_r 185,000 protein (possibly IRS-1) in MCF-7 cells.

(d) The effect of Tam on SHC was evidently different from that seen

⁴ M. Nolan, L. Jankowska, M. Prisco, S. Xu, M. Guvakova, and E. Surmacz. Differential roles of IRS-1 and SHC signaling pathways in breast cancer cells. *Int. J. Cancer*, in press.

Fig. 4. Effects of Tam on SHC signaling. The cells were grown in either PRF-SFM (SFM), PRF-SFM plus 10 nM Tam (Tam), or PRF-SFM plus 50 ng/ml IGF-1 (IGF-I) for 3 days. SHC protein were immunoprecipitated from 500 μ g of cell lysates with an anti-SHC polyclonal antibody followed by detection of tyrosine phosphorylation of SHC with PY-20. The SHC protein and SHC-associated GRB2 were detected in original filters, upon stripping and re-probing with specific antibodies. Representative results of five experiments are shown.



for IRS-1. Here, growth inhibition was associated with elevated tyrosine phosphorylation of SHC proteins, especially p52^{SHC}, without up-regulation of SHC protein levels. Importantly, long-term treatment with IGF-I, which promoted growth, concomitantly reduced SHC phosphorylation. Whether up-regulation of SHC phosphorylation is a universal feature of growth arrest or it only represents a characteristic of Tam action is presently unclear. In MCF-7 cells, treatment with genistein or herbimycin inhibited proliferation, which was associated with a reduction of SHC tyrosine phosphorylation observed after 30 min treatment (24). Longer effects of these tyrosine kinase inhibitors were not studied. In our system, higher phosphorylation of SHC in Tam-treated cells was accompanied by GRB2 binding to SHC; however, activation of ERK2 was not observed. Possibly, under Tam treatment, activation of ERK2 via SHC was counteracted by deactivation of this pathway due to disruption of IRS-1 signaling. Alternatively, as suggested by others (24, 25), the ERK2 pathway is not critical in IGF-stimulated growth in MCF-7 cells; thus, it is not a target for Tam action.

In summary, these results demonstrate that Tam differentially modulates IGF-IR signaling in breast cancer cells. The cytostatic effect of Tam is mediated by a continuing inhibition of IRS-1/PI-3 kinase pathway. On the other hand, Tam increases tyrosine phosphorylation of SHC and SHC/GRB2 binding. The biological consequences of the latter effects are presently unknown.

One possible target of Tam action is the tyrosine phosphatase system. Indeed, Freiss and Vignon (26) have recently shown that 4-hydroxytamoxifen up-regulates protein tyrosine phosphatase activity in breast cancer cells. We speculate that Tam activates, most probably through an indirect mechanism, a specific tyrosine phosphatase(s) acting upon IRS-1. On the other hand, Tam may also inhibit tyrosine phosphatase(s) that would specifically affect SHC and/or the IGF-IR. Future experiments with Tam and pure antiestrogens will further explore this issue, especially in relation with such phenomenon as antiestrogen resistance or Tam-induced growth.

References

- Lee, A. V., and Yee, D. Insulin-like growth factors and breast cancer. *Biomed. Pharmacother.*, **49**: 415-421, 1995.
- Papa, V., Gliozzo, B., Clark, G. M., McGuire, W. L., Moore, D., Fujita-Yamaguchi, Y., Vigneri, R., Goldfine, I. D., and Pezzino, V. Insulin-like growth factor I receptors are overexpressed and predict a low risk in human breast cancer. *Cancer Res.*, **53**: 3735-3740, 1993.
- Peyrat, J. P., and Bonnetterre, J. Type 1 IGF receptor in human breast diseases. *Breast Cancer Res. Treat.*, **22**: 59-68, 1992.
- Rocha, R. L., Hilsenbeck, S. G., Jackson, J. G., and Yee, D. Insulin-like growth factor binding protein-3 (IGFBP3) and insulin receptor substrate (IRS1) in primary breast cancer: larger tumors have higher BP3 levels and higher levels of IRS-1 are associated with lower disease-free survival (DFS) rate. *Breast Cancer Res. Treat.*, **37**(Suppl.): 55, 1995.
- Surmacz, E., and Burgaud, J-L. Overexpression of insulin receptor substrate 1 (IRS-1) in the human breast cancer cell line MCF-7 induces loss of estrogen requirements for growth and transformation. *Clin. Cancer Res.*, **1**: 1429-1436, 1995.
- Guvakova, M. A., and Surmacz, E. Overexpressed IGF-1 receptors reduce estrogen growth requirements, enhance survival, and promote E-cadherin-mediated cell-cell adhesion in human breast cancer cells. *Exp. Cell. Res.*, **149**-162, 1997.
- Cullen, K. J., Lippman, M. E., Chow, D., Hill, S., Rosen, N., and Zwiebel, J. A. Insulin-like growth factor-II overexpression in MCF-7 cells induces phenotypic changes associated with malignant progression. *Mol. Endocrinol.*, **6**: 91-100, 1992.
- Neuenschwander, S., Roberts, C. T., Jr., and LeRoith, D. Growth inhibition of MCF-7 breast cancer cells by stable expression of an insulin-like growth factor I receptor antisense ribonucleic acid. *Endocrinology*, **136**: 4298-4303, 1995.
- Rubin, R., and Baserga, R. Biology of disease. Insulin-like growth factor-I receptor. Its role in cell proliferation, apoptosis and tumorigenicity. *Lab. Invest.*, **73**: 311-331, 1995.
- Argetsinger, L. S., Hsu, G. W., Myers, M. G., Billestrup, N., White, M. F., and Carter-Su, C. Growth hormone, interferon- γ , and leukemia inhibitory factor promoted tyrosyl phosphorylation of IRS-1. *J. Biol. Chem.*, **270**: 14685-14692, 1995.
- Vuori, K., and Ruoslahti, E. Association of insulin receptor substrate-1 with integrins. *Science (Washington DC)*, **266**: 1576-1578, 1994.
- Pellicci, G., Lanfrancone, L., Salcini, A. E., Romano, A., Mele, S., Borrello, M. G., Segatto, O., Di Fiore, P. P., and Pellicci, P. G. Constitutive phosphorylation of Shc proteins in human cancers. *Oncogene*, **11**: 899-907, 1995.
- Habib, T., Herrera, R., and Decker, S. J. Activators of protein kinase C stimulate association of Shc and the PEST tyrosine phosphatase. *J. Biol. Chem.*, **269**: 25243-25246, 1994.
- Jordan, C. V. Molecular mechanisms of antiestrogen action in breast cancer. *Breast Cancer Res. Treat.*, **31**: 41-52, 1994.
- de Cupis, A., Noonan, D., Pirani, P., Ferrera, A., Clerico, L., and Favoni, R. E. Comparison between novel steroid-like and conventional nonsteroidal antiestrogens in inhibiting oestradiol- and IGF-I-induced proliferation of human breast cancer-derived cells. *Br. J. Pharmacol.*, **116**: 2391-2400, 1995.
- Huff, K. K., Knabbe, C., Linsey, R., Kaufman, D., Bronzert, D., Lippman, M. E., and Dickson, R. B. Multihormonal regulation of insulin-like growth factor-I-related protein in MCF-7 cells. *Mol. Endocrinol.*, **2**: 200-208, 1988.
- Colletti, R. B., Roberts, J. D., Devlin, J. T., and Copeland, K. C. Effect of tamoxifen on plasma insulin-like growth factor I in patients with breast cancer. *Cancer Res.*, **49**: 1882-1884, 1989.
- Freiss, G., Rochefort, H., and Vignon, F. Mechanisms of 4-hydroxytamoxifen anti-growth factor activity in breast cancer cells: alterations of growth factor receptor binding sites and tyrosine kinase activity. *Biochem. Biophys. Res. Commun.*, **173**: 919-926, 1990.
- Kawamura, I., Lacey, E., Mizota, T., Tsuimoto, S., Nishigaki, F., Manda, T., and Shimomura, K. The effect of droloxifen on the insulin-like growth factor-I-stimulated growth of breast cancer cells. *Anticancer Res.*, **14**: 427-432, 1994.
- Yamasaki, H., Prager, D., Gebremedhin, S., and Melmed, S. Insulin-like growth factor-I (IGF-I) attenuation of growth hormone is enhanced by overexpression of pituitary IGF-1 receptors. *Mol. Endocrinol.*, **5**: 890-896, 1991.
- Doerr, M., and Jones, J. The roles of integrins and extracellular matrix proteins in the IGF-I-stimulated chemotaxis of human breast cancer cells. *J. Biol. Chem.*, **271**: 2443-2447, 1996.
- Kleinman, D., Karas, M., Roberts, C. T., Jr., LeRoith, D., Phillip, M., Segev, Y., Levy, J., and Sharoni, Y. Modulation of insulin-like growth factor I receptors and membrane-associated IGF-I binding proteins in endometrial cancer cells by estradiol. *Endocrinology*, **136**: 2531-2537, 1995.
- Kleinman, D., Karas, M., Danilenko, M., Arbeli, A., Roberts, C. T., Jr., LeRoith, D., Levy, J., and Sharoni, Y. Stimulation of endometrial cancer cell growth by tamoxifen is associated with increased insulin-like growth factor (IGF)-I induced tyrosine phosphorylation and reduction in IGF binding proteins. *Endocrinology*, **137**: 1089-1095, 1996.
- Clark, J. W., Santos-Moore, A., Stevenson, L. E., and Frackelton, A. R., Jr. Effects of tyrosine kinase inhibitors on the proliferation of human breast cancer cell lines and proteins important in the ras signaling pathway. *Int. J. Cancer*, **65**: 186-191, 1996.
- Vinkvanwijngaarden, T., Pols, H. A. P., Buurman, C. J., Birkenhager, J. C., and Vanleeuwen, J. P. T. M. Inhibition of insulin- and insulin-like growth factor-I-stimulated growth of human breast cancer cells by 1,25-dihydroxyvitamin D-3 and the vitamin D-3 analogue EB 1089. *Eur. J. Cancer*, **32A**: 842-848, 1996.
- Freiss, G., and Vignon, F. Antiestrogens increase protein tyrosine phosphatase activity in human breast cancer cells. *Mol. Endocrinol.*, **8**: 1389-1396, 1994.

Differential roles of IRS-1 and SHC signaling pathways in breast cancer cells

Mary K. Nolan, Lidia Jankowska, Marco Prisco, Shi-qiong Xu, Marina A. Guvakova, and Ewa Surmacz*

Kimmel Cancer Institute, Thomas Jefferson University, Philadelphia, PA 19107.

Running title: IRS-1 and SHC signaling in breast cancer

*Corresponding author:

Kimmel Cancer Institute, Thomas Jefferson University
BLSB 606A, 233 S 10th Street, Philadelphia, PA 19107
Tel. 215-503-4512, FAX 215-923-0249

SUMMARY

Several polypeptide growth factors stimulate breast cancer growth and may be involved in tumor progression. However, the relative importance of diverse growth factor signaling pathways in the development and maintenance of the neoplastic phenotype is largely unknown.

The phenotype of a model breast cancer cell line MCF-7 is regulated by the activation of various growth factor receptors, for instance, the insulin-like growth factor I receptor (IGF-I R), erbB-type receptors (erbB Rs) and FGF receptors (FGF Rs). To assess the impact of two signaling molecules, insulin receptor substrate-1 (IRS-1) (a major substrate of the IGF-IR) and SHC (a substrate of different receptors such as IGF-I R, erbB-type R and FGF R), we developed several MCF-7-derived cell clones in which the synthesis of either IRS-1 or SHC was blocked by antisense RNA. In MCF-7 cells, reduction of IRS-1 by 80-85% strongly suppressed anchorage-dependent and -independent growth and induced apoptotic cell death under growth factor- and estrogen-reduced conditions. The reduction of SHC levels by approximately 50% resulted in the inhibition of monolayer and anchorage-independent growth but did not decrease cell survival. Importantly, cell-cell adhesion and the ability of cells to survive on the extracellular matrix were inhibited in MCF-7/anti-SHC clones but not in MCF-7/anti-IRS-1 clones. Cell motility towards IGF was not attenuated in any of the tested cell lines, but motility towards EGF was decreased in MCF-7/anti-SHC clones.

Thus, in MCF-7 breast cancer cells a) both IRS-1 and SHC pathways control monolayer and anchorage-independent growth; b) IRS-1 signaling plays a critical role in cell survival; c) SHC is involved in EGF-dependent motility; d) normal levels of SHC, but not IRS-1, are necessary for the formation and maintenance of cell-cell interactions.

INTRODUCTION

Several polypeptide growth factors regulate breast cancer growth and may be involved in breast cancer progression. For instance, the insulin-like growth factors I and II (IGFs), the ligands of the erbB family of receptors (erbB Rs) and fibroblast growth factors (FGFs) have been implied in breast cancer *in vitro* or *in vivo* (Dickson and Lippman, 1995). The impact of these factors on the phenotype of breast cancer cells depends on the level and activity of cognate membrane receptors. The growth of a model breast cancer cell line MCF-7, is notably enhanced by the activation of the insulin-like growth factor I receptor (IGF-IR) and the epidermal growth factor receptor (EGFR) (Dickson and Lippman, 1995, Van der Burg *et al.*, 1988, Karey and Sibrascu, 1988).

The signal transduction pathways of the IGF-IR and the EGFR share several common substrates, for example, SHC (Giorgetti *et al.*, 1994, Pelicci *et al.*, 1992). SHC proteins (p66, p52, p47) bind to the IGF-I or EGF receptors through a PTB or an SH2 domain (Tartare-Deckert *et al.*, 1995, Kavanaugh and Williams, 1994, Pelicci *et al.*, 1992). This association often results in tyrosine phosphorylation of SHC proteins, which then are able to recruit other signaling molecules, for instance GRB-type adapters, and activate downstream signaling pathways, such as Ras/MAP kinase cascade (Giorgetti *et al.*, 1994, Skolnik *et al.* 1993, Pelicci *et al.*, 1992).

The transmission of the IGF signal involves a unique element, insulin receptor substrate 1 (IRS-1), which is not implicated in EGF signaling (Myers *et al.* 1994, Rubin and Baserga, 1994). IRS-1 is a docking protein containing multiple tyrosine residues which become rapidly phosphorylated upon receptor activation. This allows association of IRS-1 with different SH2-domain containing proteins and induction of various signaling pathways, such as Ras/MAP (through an adapter GRB2), PI-3 kinase (through a p85 regulatory subunit), SHPTP2 protein tyrosine phosphatase or Jak 2 kinase (Mayers *et al.* 1994, Argesinger *et al.* 1995). Ultimately, some of the signals generated by growth factors stimulate nuclear events, while others are involved in the reorganization of cell morphology (Jones *et al.*, 1996).

The significance of IRS-1- and SHC-dependent signaling in the biology of breast tumor cells is yet not clear. Preliminary data suggest that IRS-1 may regulate the proliferation of tumor cells. In MCF-7 cells, overexpression of IRS-1 enhanced monolayer and anchorage-independent growth and reduced growth requirements for estrogen (E2) (Surmacz and Burgaud, 1995). In primary breast tumors, a correlation has been reported between the levels of IRS-1 and recurrence of the disease (Rocha *et al.*, 1995). GRB2, an adapter linking IRS-1 and SHC to Ras/MAP, is often overexpressed in breast cancer cell lines (Daly *et al.*, 1994). GRB7, a different adapter of SHC, is overexpressed and co-amplified with erbB2 in breast tumors (Stein *et al.*, 1994). The status of SHC proteins in breast cancer cell lines or tumor samples has not yet been studied.

Here, we evaluated the roles of SHC and IRS-1 in growth, survival, transformation, migration towards chemoattractants and cell-cell adhesion in breast cancer cells.

MATERIALS AND METHODS

Expression plasmids. To generate the sense and antisense-SHC expression plasmid, a 287 bp fragment of a human SHC cDNA (from nt 55 to nt 342) was amplified by PCR using the pMJ/SHC plasmid (kind gift of Dr. J. Schlessinger) as a template and oligonucleotides 5'-GTG CGG AGA CTC CAT GAG-3' and 5'-CTC ACA CAC CAG ACT GAT G-3', as the upstream and downstream primer, respectively. The amplified SHC DNA fragment was cloned into the pCR3 expression plasmid (Invitrogen) in either 5'-3' or 3'-5' orientation to produce sense-SHC or antisense-SHC expression vectors (respectively). In the resulting expression vectors, transcription of sense or antisense-SHC RNA was driven by CMV promoter. The expression plasmids also encoded neomycin resistance to allow for selection in G418.

The antisense and sense-IRS-1 expression plasmids have been described previously (D'Ambrosio *et al.*, 1995). The plasmids contain the entire sequence of mouse IRS-1 cDNA cloned in either the sense or antisense direction in pRc/CMV expression vector (Invitrogen).

Cell lines and cell culture conditions. MCF-7/antisense-SHC (anti-SHC) and MCF-7/antisense-IRS-1 (anti-IRS-1) clones were generated by stable transfection using calcium phosphate precipitation method. The clones were selected in 2 mg/ml G418, and the integration of transfected plasmids into genomic DNA was confirmed by PCR. In all cases, a "T7 primer" 5'-CGA CTC ACT ATA GG-3' (located in the T7 promoter of all expression plasmids) was used as an upstream primer. The following downstream primers were used: for sense IRS-1 clones: 5'-GGC TTC TCA GAC GTG CGC AAG-3'; for antisense IRS-1 clones: 5'-GAT AAC TGC TAG GAG ACC-3'; for sense SHC clones: 5'-CTC ACA CAC CAG ACT GAT G-3'; for antisense SHC clones: 5'-CTG CGG AGA CTC CAT GAG-3'. From each transfection, 13 PCR-positive clones were tested for the levels of target protein by Western immunoblotting (see below).

Cells were maintained in DMEM : F12 supplemented with 5% calf serum (CS). In the experiments requiring growth factor- and estrogen-reduced conditions, we used DMEM without phenol red (PRF-DMEM) with 0.5 mg/ml BSA, 1 μ M FeSO₄ and 2 mM L-glutamine (PRF-serum free media, PRF-SFM).

Western blotting. Reduction of SHC and IRS-1 protein levels in MCF-7 clones was confirmed by Western immunoblotting. In MCF-7/anti-IRS-1 clones, cell lysates (1.5 mg) were immunoprecipitated with an anti-IRS-1 antibody (UBI) and probed with another anti-IRS-1 antibody (obtained from Dr. M. Myers, Joslin Diabetes Center, Boston, MA). The same method was used to assess the levels of IRS-1 in MCF-7/anti-SHC clones, except that 500 μ g of protein lysate were used for immunoprecipitation.

In MCF-7/anti-SHC and MCF-7/anti-IRS-1 clones, 50 μ g of total cell lysate were resolved by PAGE, and SHC proteins were immunodetected with an anti-SHC monoclonal antibody (Transduction Laboratories). The levels of IRS-1 and SHC proteins were approximated by laser densitometry reading.

Anchorage-dependent growth assay. Cells were plated at a concentration $1 \times 10^5/30$ mm well in DMEM : F12 supplemented with 5% CS. After 24 h, the cells were washed 3 times with PRF-DMEM and the media was replaced with either PRF-SFM, PRF-SFM containing 20 ng/ml IGF-I, or PRF-SFM with 5 ng/ml EGF. At day 0 (media change) and day 2, the number of cells was determined by direct cell counting with trypan blue exclusion.

Anchorage-independent growth assay. This assay was performed as previously described (Sell *et al.*, 1993). Briefly, the cells were plated at a concentration of $5 \times 10^3/30$ mm plate in DMEM with 10% FBS (fetal bovine serum) solidified with 0.2% agarose. DMEM with 10% FBS plus 0.4% agarose was used as underlay. After 3 weeks, colonies greater than 150 μ m were counted.

Apoptosis analysis. Flow cytometry cell sorting (FACS): At time 0, or after 24 h incubation in PRF-SFM media, cells were washed with cold PBS and fixed by the addition of 70% ice-cold ethanol. Following another wash in PBS, the cells were treated with RNase (75 μ g/ml) for 30 min at 37°C, washed again in PBS and then resuspended in PBS containing 15 μ g/ml propidium iodide. A minimum of 2×10^4 cells was analyzed by FACS with a Coulter Epics Profile II (Coulter Electronics, Inc., Hialeah, FL).

In situ detection of apoptosis: Apoptotic cells were identified with the TACS/Blue Label in situ apoptotic detection kit (Trevigen) following manufactures protocol. Briefly, the cells were plated on glass slides in 100 mm plates and grown till 70% confluence. Then, the cultures were washed 3 times with PRF-DMEM and shifted to PRF-SFM for 24 h. Next, the cells were fixed in 3.7% paraformaldehyde and treated first with protease and then with H₂O₂ (to remove exogenous peroxidase). In situ labeling of fragmented DNA was performed with Klenow enzyme in the presence of labeled oligodeoxynucleotides. Labeled DNA was visualized with Blue Label, followed by counterstaining with Red Counterstain B. For each experimental condition, at least 1×10^3 cells were counted and apoptosis was determined based on specific staining and cell morphology.

Cell aggregation assay. This assay has been performed as described by us before (Guvakova and Surmacz, in press). Briefly, Matrigel (extracellular matrix) (Biocoat/Fisher) was reconstituted according to the manufactures instruction. Cells were plated at 2×10^4 cells/well in 24-well plates coated with 200 μ l of Matrigel. After 6 days, the number and size of aggregates were counted and measured, and the cultures were

photographed. To determine the number of viable cells, the aggregates were dissociated from the matrix during a 2 h incubation in Dispase (Biocoat/Fisher) at 37° C and the cells were counted with trypan blue exclusion.

Cell motility assay. Cell motility was tested using Transwell polycarbonate membrane inserts with an 0.8 μ m pore size (Costar) as described before (Doerr and Jones, 1996). The cells were plated in DMEM : F12 plus 5% CS at a concentration of 2×10^4 cells/insert. The inserts were placed in wells containing either DMEM : F12 plus 5% CS (controls), or DMEM : F12 plus 5% CS supplemented with either 20 ng/ml IGF-I or 5 ng/ml EGF. After a 16 h incubation, the cells that traversed through the pores and attached to the underside of the insert were stained with Comassie blue. The number of cells was determined by direct cell counting.

RESULTS

Development of MCF-7/anti-IRS-1 and MCF-7/anti-SHC clones. To compare the importance of IRS-1- and SHC-dependent signaling pathways in MCF-7 breast cancer cells, we developed several MCF-7-derived clones expressing antisense RNA to either IRS-1 or SHC. In MCF-7/anti-IRS-1 clones, the level of IRS-1 was reduced up to 85%, whereas in MCF-7/anti-SHC clones, up to 55% inhibition of target protein expression was observed. Interestingly, in both cases, we did not obtain clones with an intermediate (25-40%) degree of reduction. In fact, the majority of PCR-positive clones exhibited either none or a very modest (up to 15%) down-regulation of IRS-1 or SHC.

The levels of IRS-1 and SHC in several clones with the best inhibition of target protein expression demonstrates Fig. 1. In MCF-7/anti-IRS-1, clones 9, 2 and 1, the levels of IRS-1 were reduced by 85% and 80% and 70%, respectively (Fig. 1A). In MCF-7/anti-SHC clones 12, 4 and 2, SHC expression (both p47 and p52) was inhibited by 47%, 50% and 55%, respectively (Fig. 1B). Notably, p66 SHC was not detectable in either of the MCF-7-derived cell lines, which confirmed our previous findings (Guvakova and Surmacz, in press).

To control for specificity of antisense RNA activity, we measured the amounts of IRS-1 in MCF-7/anti-SHC clones and, conversely, the levels of SHC in MCF-7/anti-IRS-1 clones. The amounts of IRS-1 in all MCF-7/anti-SHC clones and MCF-7 cells were similar, with a variation of $\pm 12\%$. Also, the levels of SHC were comparable in MCF-7/anti-IRS-1 clones and MCF-7 cells, with a variation of $\pm 15\%$ (Fig. 1A and B, lower panels).

Two MCF-7/anti-IRS-1 clones (2 and 9) and two MCF-7/antisense SHC clones (2 and 4), with the best inhibition of target protein, were selected for further experiments.

MCF-7 cells with reduced levels of IRS-1 or SHC exhibit inhibition of monolayer growth. The ability of MCF-7/anti-SHC and MCF-7/anti-IRS-1 clones to grow in monolayer culture was tested under four different conditions: DMEM : F12 plus 5% CS, PRF-SFM, PRF-SFM plus 20 ng/ml IGF-I, or PRF-SFM plus 5 ng/ml EGF. The treatments with IGF-I and EGF were chosen because, out of the many growth factors tested, these were the best mitogens for MCF-7 cells cultured in our laboratory (data not shown). Moreover, the fact that SHC is activated by IGF-I and EGF, whereas IRS-1 is a substrate of the IGF-IR, but not the EGFR, provided additional differentiating condition in testing the antisense clones. Several control cell lines were used in these studies: the parental MCF-7 cells, MCF-7/pc4 cells transfected with an empty vector (described by Guvakova and Surmacz, in press) and MCF-7/IRS-1 cells, which overexpress IRS-1 and exhibit amplification of IGF signaling (characterized in detail by Surmacz and Burgaud, 1995). Fig. 2 summarizes the obtained data. The increase of the number of MCF-7 cells under given condition was taken as 100%; the increase of the number of tested cells was calculated relative to MCF-7 cells. The growth was defined as increase in the number of viable cells. It should be noted that MCF-7 cells secrete IGF-like mitogens (Surmacz and Burgaud, 1995), therefore all experimental conditions included additional IGF-like autocrine factors.

In medium containing 5% CS (Fig. 2), the proliferation of MCF-7/anti-SHC clones was significantly inhibited. Specifically, compared with the parental cells, the growth was

reduced by 55% (clone 2) and 27% (clone 4). Similarly, in MCF-7/anti-IRS-1 cells, the viable cell number was decreased by 61% (clone 2) and 57% (clone 9).

In PRF-SFM (Fig. 2), despite the presence of IGF-like autocrine factors, a large population of MCF-7/anti-IRS-1 cells was dying. In fact, compared with MCF-7 cells, the viable cell number was decreased by 142% (clone 2) and 130% (clone 9). Under the same conditions, MCF-7/anti-SHC clones survived better, although their growth was inhibited by 60% (clone 2) and 93% (clone 4).

Similar results were obtained in PRF-SFM supplemented with 20 ng/ml IGF (Fig. 2). Here, the growth of MCF-7/anti-SHC clones was inhibited by 67% (clone 2) and 83% (clone 4). Under these conditions, MCF-7/anti-IRS-1 cells were massively dying; relative to MCF-7 cells, a 145% (clone 2) and 148% (clone 9) decrease in cell number was noted.

In PRF-SFM supplemented with 5 ng/ml EGF (Figure 2D), MCF-7/anti-SHC clones were inhibited by 82% (clone 2) and 74% (clone 4), while in MCF-7/anti-IRS-1 clones a 75% (clone 2) and 41% (clone 9) growth decrease was obtained.

The control cells, MCF-7/sense-SHC and MCF-7/pc4, grew similar to MCF-7 cells under all tested conditions. MCF-7/IRS-1 cells exhibited increased responsiveness to IGF-I and EGF, compared with the parental cell line, consistent with the previously published data (Surmacz and Burgaud, 1995).

In all tested cell lines, mitogenic response to E2 was similar (data not shown).

MCF-7/anti-IRS-1 cells undergo apoptosis under serum-free conditions. To determine the mechanism of cell death apparent in monolayer growth in PRF-SFM and PRF-SFM plus IGF-I, the clones were analyzed for evidence of apoptosis. Two independent methods were employed, in situ detection of fragmented DNA and FACS analysis.

In growing cells (time 0), apoptosis was identified in a small fraction of all tested cell lines (Tab. 1). In contrast, after 24 h culture in growth factor- and estrogen-reduced conditions, the rate of apoptosis significantly increased in MCF-7/anti-IRS-1 cells, up to 39.6%, but not in MCF-7/anti-SHC cells or other cell lines. Similar results were obtained after 48 h culture in PRF-SFM (data not shown).

The higher incidence of apoptotic cell death in MCF-7/anti-IRS-1 clones was confirmed with FACS analysis, in which a pre-G1 peak, possibly representing the population of apoptotic cells, was observed (Fig. 3). The peak was not detectable in MCF-7 cells (Fig. 3) and MCF-7/anti-SHC clones (data not shown).

Anchorage-independent growth is blocked in MCF-7/anti-IRS-1 and MCF-7/anti-SHC cells. The overexpression of IRS-1 has been shown to enhance anchorage-independent growth in MCF-7 cells (Surmacz and Burgaud, 1995). Amplification of SHC promoted transforming abilities in fibroblasts (Pelicci *et al.*, 1992). Here, we tested anchorage-independent growth (colony formation in soft agar) of MCF-7/anti-IRS-1 and MCF-7/anti-SHC clones (Tab. 2). In both cases, we found that colony formation was similarly inhibited, by at least 72%, when compared with MCF-7 cells. The anchorage-independent growth of different control cell lines was comparable to that of MCF-7 cells.

MCF-7/anti-SHC clones exhibit impaired aggregation and survival on the extracellular matrix. Our previous studies indicated that overexpression of the IGF-IR in MCF-7 cells dramatically increased the ability of cells to aggregate on the extracellular matrix (ECM) (Guvakova and Surmacz, in press). Moreover, the formation of multiple cell-cell contacts supported proliferation of clustered cells and possibly decreased the rate of cell death. Consequently, we studied the effects of blocking SHC or IRS-1 signaling pathway on cell-cell adhesion.

The experiments demonstrated that while MCF-7/anti-IRS-1 clones were able to aggregate on ECM to a similar extent as control cell lines (MCF-7 and MCF-7/sense SHC cells), the aggregation of both MCF-7/anti-SHC clones was clearly inhibited (Fig. 4). Specifically, MCF-7, MCF-7/sense SHC cells and MCF-7/anti-IRS-1 clones produced only large clusters ranging in size from 230 to 300 μ m, whereas MCF-7/anti-SHC clones formed small aggregates (approximately 50 μ m in diameter). Furthermore, in the case of clones that formed large aggregates (MCF-7, MCF-7/sense SHC and MCF-7/anti-IRS-1

cells) were also able to survive on ECM up to 7 days. In contrast, the population of viable MCF-7/anti-SHC cells was reduced by at least 50% during this time (Tab. 3)

EGF-dependent cell motility is affected in by the reduction of SHC levels in MCF-7 cells. The IGF-IR has been shown to mediate motility in breast cancer cells (Doerr and Jones, 1996). We studied the ability of MCF-7/anti-IRS-1 and MCF-7/anti-SHC cells to migrate toward a chemoattractant, IGF or EGF (Tab. 4). Both IGF-I and EGF stimulated the motility of all studied cell lines. The tendencies to migrate towards IGF were similar for all studied cells, however some clonal variations were observed (64-95% increase over basal migration in growth medium). However, when EGF was used as an chemoattractant, in MCF-7 cells, MCF-7/IRS-1 and MCF-7/sense-SHC clones, as well as in both MCF-7/anti-IRS-1 clones, migration increased by 28-56% over that stimulated by IGF (Tab. 4). In contrast, migration of MCF-7/anti-SHC clones towards EGF was decreased by 32% (clone 2) and 70% (clone 4) compared with IGF stimulation. In all cases, the differences between IGF-I and EGF chemoattraction were statistically significant ($p < 0.05$, by ANOVA).

DISCUSSION:

Although it is known that polypeptide growth factors, such as the IGFs and the ligands of the erbB family of receptors, play an important role in the regulation of breast cancer growth and progression, the functions of different signaling pathways in the development of a neoplastic phenotype has not been elucidated (Dickson and Lippman, 1995). We have addressed the role of two signaling elements, IRS-1, a major substrate of the IGF-IR (but also involved in insulin and IL4 signaling)(Myers *et al.*, 1994) and SHC, an important substrate of different tyrosine kinase receptors, e.g., the IGF-IR and erbB-type Rs (Sepp-Lorenzino *et al.*, 1996, Giorgetti *et al.*, 1994, Pelicci *et al.*, 1992). Since previous studies have demonstrated growth inhibition in MCF-7 cells stably expressing an IGF-IR antisense RNA (Neuenschwander *et al.*, 1995), we have used an antisense RNA approach to generate MCF-7 cell lines expressing reduced levels of either IRS-1 or SHC. The developed antisense clones were tested for their ability to grow under anchorage-dependent and -independent conditions, to survive in estrogen- and growth factor-reduced media, to migrate towards chemoattractants and to maintain cell-cell interactions.

The major finding of this work are: 1) In MCF-7 cells, IRS-1 and SHC signaling pathways are necessary to support monolayer and anchorage-independent growth; 2) significant reduction of IRS-1 levels induces cell death; 3) reduction of SHC levels, but not IRS-1 levels, affects cell-cell interactions on extracellular matrix; 4) decrease of SHC levels impairs EGF-, but not IGF-I-stimulated migration of MCF-7 breast cancer cells.

The most striking differences between MCF-7/anti-IRS-1 and MCF-7/anti-SHC clones were seen in cell aggregation on Matrigel. The results suggested that normal amounts of SHC, but not IRS-1, are required for the formation and maintenance of cell-cell contacts. Our previous studies demonstrated that in MCF-7 cells, E-cadherin-dependent cell-cell adhesion is significantly enhanced by the overexpression of the IGF-IR. Additionally, the IGF-IR and its substrates, IRS-1 and SHC, were associated with E-cadherin (Guvakova and Surmacz, in press). The mechanism of IGF-I stimulated adhesion in breast epithelial cells is still unclear (Guvakova and Surmacz, in press, Bracke *et al.*, 1993) but based on the present work, a role of SHC signaling could be suggested. The involvement of SHC in cell-cell interactions is also supported by the recent finding of the direct association of SHC and N-cadherin *in vitro* (Xu *et al.*, 1996).

Remarkably, in MCF-7 cells, down-regulation of IRS-1 levels, which was sufficient to inhibit growth in monolayer culture and in soft agar, did not affect cell aggregation and only moderately (20%) inhibited cell survival on Matrigel. A limited role of IRS-1 in cell-cell adhesion was confirmed by the experiments with MCF-7/IRS-1 cells, overexpressing approximately 10-fold IRS-1 (Surmacz and Burgaud, 1995), in which no significant induction of aggregation, compared with that of MCF-7 cells, was obtained (manuscript in preparation). The survival of clustered MCF-7/IRS-1 cells, however, was enhanced, which may suggest an important role of IRS-signaling in protection from cell death.

The possible function of IRS-1 in survival of MCF-7 cells was also demonstrated in monolayer growth experiments. In PRF-SFM and PRF-SFM with IGF-I, MCF-7/anti-IRS-1 cells were massively dying. This suggested that other pathways activated under these conditions, for instance SHC, did not provide sufficient signal for survival and could not compensate for IRS-1 loss. Importantly, in anti-IRS-1 clones, cell death was executed through apoptosis. Apoptosis was detected by FACS and in situ labeling, the methods of choice for breast epithelial cells in which an apoptotic DNA ladder usually is not detectable (Wilson *et al.*, 1995). Apoptosis was not identified in cells with normal IRS-1 amounts, for instance, in MCF-7 cells or in anti-SHC clones growing in the presence of IGF (autocrine or exogenous). Interestingly, when anti-IRS-1 clones were cultured in media supplemented with CS or EGF, the cells were able to survive, probably because other than IRS-1-dependent survival mechanisms were operative under these conditions. For example, a PI-3 kinase pathway (which can be activated by, for instance, the EGFR) has been found to control cell survival (Parrizas and LeRoith, in press).

The role of SHC in survival of MCF-7 cells is difficult to evaluate, partly because in our model, reduction of SHC levels was not as significant as that of IRS-1 levels. The inhibition of SHC by approximately 60% was not sufficient to induce cell death in monolayer culture, even in PRF-SFM. Thus, in MCF-7 cells, normal amounts of SHC were not essential for survival in monolayer culture. However, the survival of cells on Matrigel (in the presence of different growth factors) was inhibited in MCF-7/anti-SHC clones. We speculate that this represented a secondary effect to impaired cell aggregation in these cells, since aggregation itself has been shown to promote survival on Matrigel (Guvakova and Surmacz, in press).

The studies of anchorage-dependent growth additionally suggested the important function of both SHC and IRS-1 in proliferation. In MCF-7/anti-IRS-1 and MCF-7/anti-SHC clones, cell growth was blocked even in medium containing CS. This reflected mostly the inhibition of proliferation, since, even in MCF-7/anti-IRS-1 cells, only minimal cell death was observed (Tab 1 and unpublished observations). Similar results were obtained in medium supplemented with EGF (naturally containing autocrine IGF-like factors and possibly other unidentified mitogens) (Fig. 2).

The greatest level of growth reduction, for both MCF-7/anti-IRS-1 and MCF-7/anti-SHC, was seen in SFM containing only IGF (autocrine or exogenous). The results suggested that normal levels of either IRS-1 or SHC were not sufficient to sustain growth in IGF when the other pathway was impaired. Therefore, both pathways regulate IGF-I-dependent monolayer growth of MCF-7 cells.

We previously demonstrated that IRS-1 is required for growth in soft agar in MCF-7 cells and in other cell models (Surmacz and Burgaud, 1995, D'Ambrosio *et al.*, 1995). In mouse fibroblasts, SHC was implicated in the control of cellular transformation (Pelicci *et al.*, 1992). We confirmed that both SHC and IRS-1 are critical elements regulating anchorage independent growth in MCF-7 cells. In our model, colony formation in both MCF-7/anti-SHC and MCF-7/anti-IRS-1 clones was significantly (by at least 70%) inhibited, compared with control cell lines expressing normal amounts of both substrates (Tab. 2).

It has been shown that in different breast cancer cell lines, motility is stimulated by the activation of the IGF-IR (Doerr and Jones, 1996). Our results did confirm that IGF-I stimulates migration of MCF-7 cells. We also found that in MCF-7 cells migration was stimulated by EGF. Contrary to the other report (Doerr and Jones, 1996), in our hands, EGF was a significantly better chemoattractant for the studied cells than IGF. The reason for this discrepancy is not clear. It is possible that the subline of MCF-7 cells cultured in our laboratory differs from the one described by others, in particular our MCF-7 cells were able to traverse only uncoated membranes, whereas the cells described by Doerr and Jones (1996) invaded through either gelatin, laminin or collagen.

Under our experimental conditions, IGF-I-dependent migration was similar in all tested cell lines and was not evidently inhibited in either MCF-7/anti-SHC or MCF-7/anti-IRS-1 clones. It is possible that the IGF-IR activated other pathways providing sufficient signal for migration, or alternatively, the inhibition of either IRS-1 or SHC signaling was too modest to inhibit migration. Noteworthy, the EGF-stimulated motility was significantly

blocked in MCF-7/anti-SHC clones. Thus, SHC may act as a critical signaling substrate of the EGFR-regulated migration in MCF-7 cells.

In summary, our work suggested differential roles for IRS-1 and SHC signaling pathways in MCF-7 cells. The studies of normal and cancer cell lines overexpressing these and other substrates as well as the analysis of signaling molecules in tumor samples, should provide additional information on the development of a neoplastic phenotype in breast epithelial cells.

ACKNOWLEDGMENTS. Blue Label used for detection of apoptotic cells was a generous gift of Dr. Philip Vanek (Trevigen). This work was supported in part by the grant NIH DK48969 (E.S). E.S is a recipient of Career Development Award (TR 950198) from the Department of the Army.

REFERENCES

- ARGETSINGER, L.S. HSU, G.W., MYERS, M.G., BILLESTRUP, N., WHITE, M.F., and CARTER-SU, C. Growth hormone, interferon-gamma, and leukemia inhibitory factor promoted tyrosyl phosphorylation of IRS-1. *J. Biol. Chem.* 270: 14685-14692 (1995)
- BRACKE, M. E., VYNCKE, B. M., BRUYNEEL, E. A., VERMEULEN, S. J., DE BRUYNE, G. K., VAN LAREBEKE, N A., VLEMINCK, K., VAN ROY, F. M., and MAREEL, M. M. Insulin-like growth factor I activates the invasion suppressor function of E-cadherin in MCF-7 human mammary carcinoma cells in vitro. *Br. J. Cancer.* 68: 282-289 (1993).
- D'AMBROSIO, C., KELLER, S.R., MORRIONE, A., LIENHARD, G.E., BASERGA, R., and SURMACZ, E. Transforming potential of the insulin receptor substrate 1. *Cell Growth Diff.* 6:557-562 (1995)
- DALY, R. J., BINDER, M. D., and SUTHERLAND, R. L. Overexpression of GRB2 gene in human breast cancer cell lines. *Oncogene* 9: 2723-2727 (1994)
- DICKSON R., B., and LIPPMAN, M. E. Growth factors in breast cancer. *Endocrine Rev.* 16: 559-589 (1995)
- DOERR, M., and JONES, J. The roles of integrins and extracellular matrix proteins in the IGF-I-stimulated chemotaxis of human breast cancer cells. *J. Biol. Chem.* 271: 2443-2447 (1996)
- GIORGETTI, S., PELICCI, P.G., PELICCI, G., and VAN OBERGHEN, E. Involvement of Src-homology/collagen (SHC) proteins in signaling through the insulin receptor and the insulin-like growth factor-I receptor. *Eur. J. Bioch.* 223: 195-202 (1994).
- GUVAKOVA, M., and SURMACZ, E. Overexpressed IGF-IR reduce IGF-I and estrogen growth requirements, enhance survival and promote E-cadherin-mediated cell-cell adhesion in human breast cancer cells. *Exp. Cell Res.* in press
- JONESON, T., WHITE, M. A., WIGLER, M. H., BAR-SAGI, D. Stimulation of membrane ruffling and MAP kinase activation by distinct effectors of RAS. *Science* 271: 810-812 (1996)
- KAREY K. P., and SIBRASCU, P. A. Differential responsiveness of human breast cancer cell lines MCF-7 and T47 D to growth factors and 17-beta estradiol. *Cancer Res.* 98: 4089-4092 (1988)
- KAVANAUGH, and W.M. WILLIAMS, L.T. An alternative to Sh2 domains for binding tyrosine-phosphorylated proteins. *Science* 266: 1862-1864 (1994).

- MYERS, M., SUN, X.J., and WHITE, M. The IRS-1 signaling system. *TIBS* 19: 289-293 (1994).
- NEUENSCHWANDER, S., ROBERTS, C.T., and LEROITH, D. Growth inhibition of MCF-7 breast cancer cells by stable expression of an insulin-like growth factor I receptor antisense ribonucleic acid. *Endocrinology* 136: 4298-42303 (1995)
- PARRIZAS, M., SALTIEL, A., and LeROITH D. IGF-I inhibits apoptosis using the PI-3 kinase pathway and the Map kinase pathway. *J. Biol. Chem.* in press
- PELICCI, G., LANFRANCONE, L., GRIGNANI, F., MCGLADE, J., CAVAOOL, F., FORNI, G., NICOLETTI, I., GRIGNANI, F., PAWSON, T., and PELICCI, P.G. A novel transforming protein (SHC) with an SH2 domain is implicated in mitogenic signal transduction. *Cell* 70: 93-104 (1992).
- ROCHA, R. L., HILSENBECK, S. G., JACKSON, J. G., and YEE, D. Insulin-like growth factor binding protein-3 (IGFBP3) and insulin receptor substrate 1 (IRS1) in primary breast cancer: larger tumors have higher BP3 levels and higher levels of IRS-1 are associated with lower disease-free survival (DFS) rate. *Breast Cancer Res. Treatm. Suppl.* 37: 55 (1995)
- RUBIN, R., and BASERGA, R. Biology of disease. IGF-IR. Its role in cell proliferation, apoptosis and tumorigenicity. *Lab Invest.* 73: 311-331 (1995).
- SELL, C., RUBINI, R., LIU, J.P. EFSTRATIADIS, A., and BASERGA, R. Simian virus 40 large tumor antigen is unable to transform mouse embryonic fibroblasts lacking type-1 IGF receptor. *Proc. Natl. Acad. Sci USA*, 90: 11217-11221 (1993)
- SEPP-LORENZINO, L., EBERHARD, I., MA, Z., CHO, C., SERVE, H., LIU, F., ROSEN, N., and LUPU, R. Signal transduction pathways induced by heregulin in MDA-MB-453 breast cancer cells. *Oncogene* 12: 1679-1687 (1996)
- SKOLNIK, E.Y., LEE, C.H., BATZER, A., VICENTINI, L.M. ZHOU, M., DALY, R., MYERS, M.J., BACKER, J.M. ULRICH, A., WHITE, M.F., and SCHLESSINGER, J. The SH2/SH3 domain containing protein GRB2 interacts with tyrosine-phosphorylation IRS-1 and SHC: implications for control of ras signaling. *EMBO J.* 12: 1929-1936 (1993).
- STEIN, D., WU, J., FUQUA, S. A., ROONPRAPUNT, C., YAJNIK. V., D'EUSTACHIO, P., MOSKOW, J. J., BUCHBERG, A. M., OSBORNE, C. K., and MARGOLIS, B. The SH2 domain protein GRB-7 is co-amplified, overexpressed and in a tight complex with HER2 in breast cancer. *EMBO J.* 13: 1331-1340 (1994)
- SURMACZ, E., and BURGAUD, J.L. Overexpression of IRS-1 in the human breast cancer cell line MCF-7 induces loss of estrogen requirements for growth and transformation. *Clin. Cancer Res.* 1: 1429-1436 (1995)
- TARTARE-DECKERT, S., SAWKA-VERHELLE, D., MURDACA, J., and VAN OBBERGHEN, E. Evidence for differential interaction of SHC and the IRS-1 with the IGF-IR in the yeast two-hybrid system. *J. Biol. Chem.* 270:23456-23460 (1995).
- VAN DER BURG, B., RUTTEMAN, G. R., BLANKENSTEIN, M. A., DE LATT S., W., and VAN ZOELLEN E. J. J. Mitogenic stimulation of human breast cancer cells in growth factor-defined medium: synerfistic action of insulin and estrogen. *J. Cell Physiol.* 134: 101-108 (1988)
- WILSON, W. W., WAKELING, A. E., MORRIS, I. D., HICKMAN J. A. and DIVE, C. MCF-7 human mammary adenocarcinoma cell death in vitro in response to hormone-withdrawal and DNA damage. *Int. J. Cancer* 61: 502-508 (1995).

XU, Y., GUO, D. F., DAVIDSON, M., INAGAMI, T., and CARPENTER, G. In vitro interaction of adapter protein SHC with cell adhesion molecule cadherin. *Mol. Biol. Cell.* 7: 342a (1996).

Table 1. Apoptosis in MCF-7/anti-IRS-1 and MCF-7/anti-SHC cells.

Cell lines	Apoptotic cells (%)	
	0 h	24 h
MCF-7	0.8±0.5	3.0±0.8
MCF-7/pc4	0.5±0.1	1.9±0.1
MCF-7/IRS	1.2±0.7	3.7±1.1
MCF-7/anti-IRS-1, 2	1.9±0.8	22.5±2.3
MCF-7/anti-IRS-1, 9	4.3±1.2	39.6±1.4
MCF-7/anti-SHC, 2	1.2±0.8	1.5±0.3
MCF-7/anti-SHC, 4	0.8±0.1	3.6±0.5
MCF-7/sense-SHC	2.0±0.2	2.3±0.0

DNA fragmentation in situ was detected using a Trevigen in situ detection kit following manufacturers methodology, as described under Materials and Methods. The results shown are means ±SD from at least 3 independent experiments.

Table 2. Anchorage-independent growth of MCF-7/anti-IRS-1 and MCF-7/anti-SHC cells.

Cell Line	No of Colonies	Inhibition (%)
MCF-7	101±5.9	-
MCF-7/pc4	98±1.0	3
MCF-7/anti-IRS1, 2	14±6.7	86
MCF-7/anti-IRS-1, 9	28±4.5	72
MCF-7/anti-SHC, 2	12±3.5	88
MCF-7/anti-SHC, 4	28±6.0	72
MCF-7/sense SHC	103±9.4	-

Cells were plated in soft agar in 10% FBS at 5×10^5 cells/plate. Colonies greater than 150 μ m were counted after 3 weeks. The data are means ± SD from 3 independent experiments.

Table 3. Survival of MCF-7/anti-IRS-1 and MCF-7/anti-SHC clones on Matrigel.

Cell Lines	No of Cells at Day 6
MCF-7	19,300±818
MCF-7/pc4	17,266±1,010
MCF-7/anti-IRS-1, 2	18,233±709
MCF-7/anti-IRS-1, 9	18,366±1,517
MCF-7/anti-SHC, 2	6,000±1,000
MCF-7/anti-SHC, 4	9,500±1,040
MCF-7/sense SHC	19,333±1,527

Cells were at 2×10^4 /well in 24-well plates on Matrigel Matrix (Biocoat/Fisher). On day 6, the number of cells was determined by direct cell counting with trypan blue exclusion after dissociation of aggregates by dispase at 37°C for 2 h. The data are means ±SD from at least 3 independent experiments.

Table 4. Motility of MCF-7/anti-IRS-1 and MCF-7/anti-SHC cells

Cell Line	Chemoattraction	
	IGF	EGF
	(% over Basal)	
MCF-7	195±7.2	245±7.1
MCF-7/IRS-1	186±6.1	217±2.5
MCF-7/sense SHC	167±6.1	212±10.0
MCF-7/anti-IRS-1, 2	164±3.0	194±2.6
MCF-7/anti-IRS-1, 9	165±5.0	195±9.0
MCF-7/anti-SHC, 2	175±2.0	148±5.9
MCF-7/anti-SHC, 4	195±8.6	128±7.0

Cells (2×10^4) suspended in growth medium were plated in Transwell inserts and the migration towards IGF or EGF was evaluated as described under Methods. Migration towards growth medium was taken as basal. The data are average \pm SD from at least 3 independent experiments.

FIGURE LEGENDS

Figure 1. Levels of IRS-1 and SHC in the developed clones. The levels of target proteins in MCF-7/anti-IRS-1 cells (A) and MCF-7/anti-SHC cells (B) and control cell lines were immunodetected as described under Materials and Methods.

Figure 2. Anchorage-dependent growth. Ordinate, relative % increase in cell number with the increase of MCF-7 cells taken as 100%. Abscissa, cell lines tested.

Figure 3. Apoptosis analysis. To identify apoptosis in MCF-7 cells and MCF-7/anti-IRS-1 clones 2 and 9, FACS analysis was performed with a Coulter Epics Profile II as described under Methods.

Figure 4. Cell aggregation on Matrigel. Representative picture of cell aggregation in tested cell lines. The aggregation was tested as described under Methods; cells were photographed with 100x magnification at day 5 of the experiment.

FIG. 1

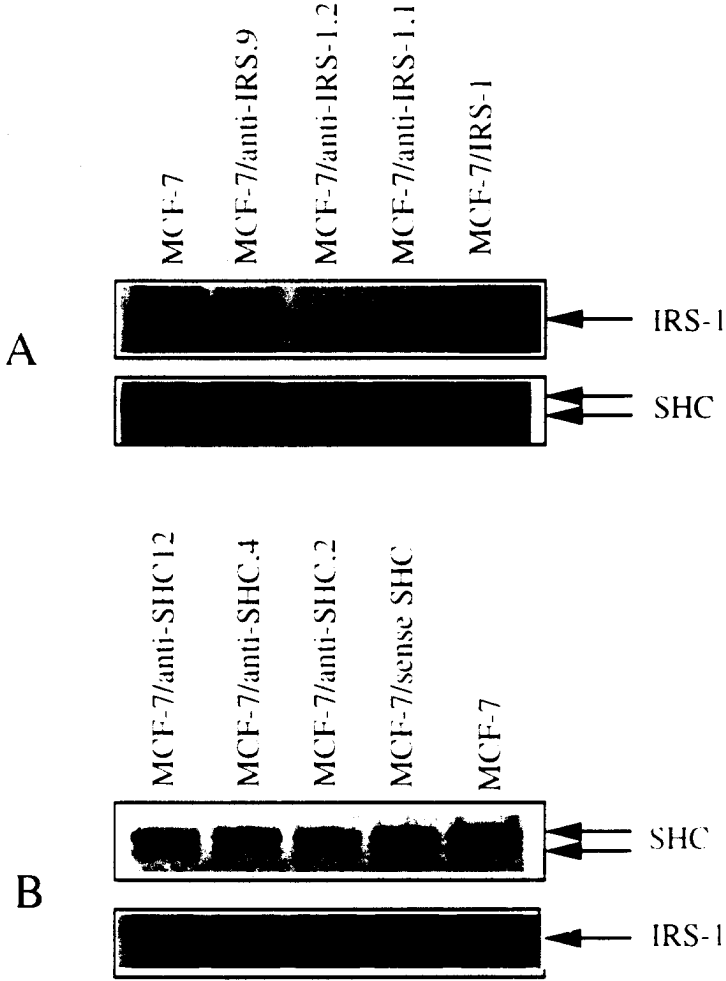
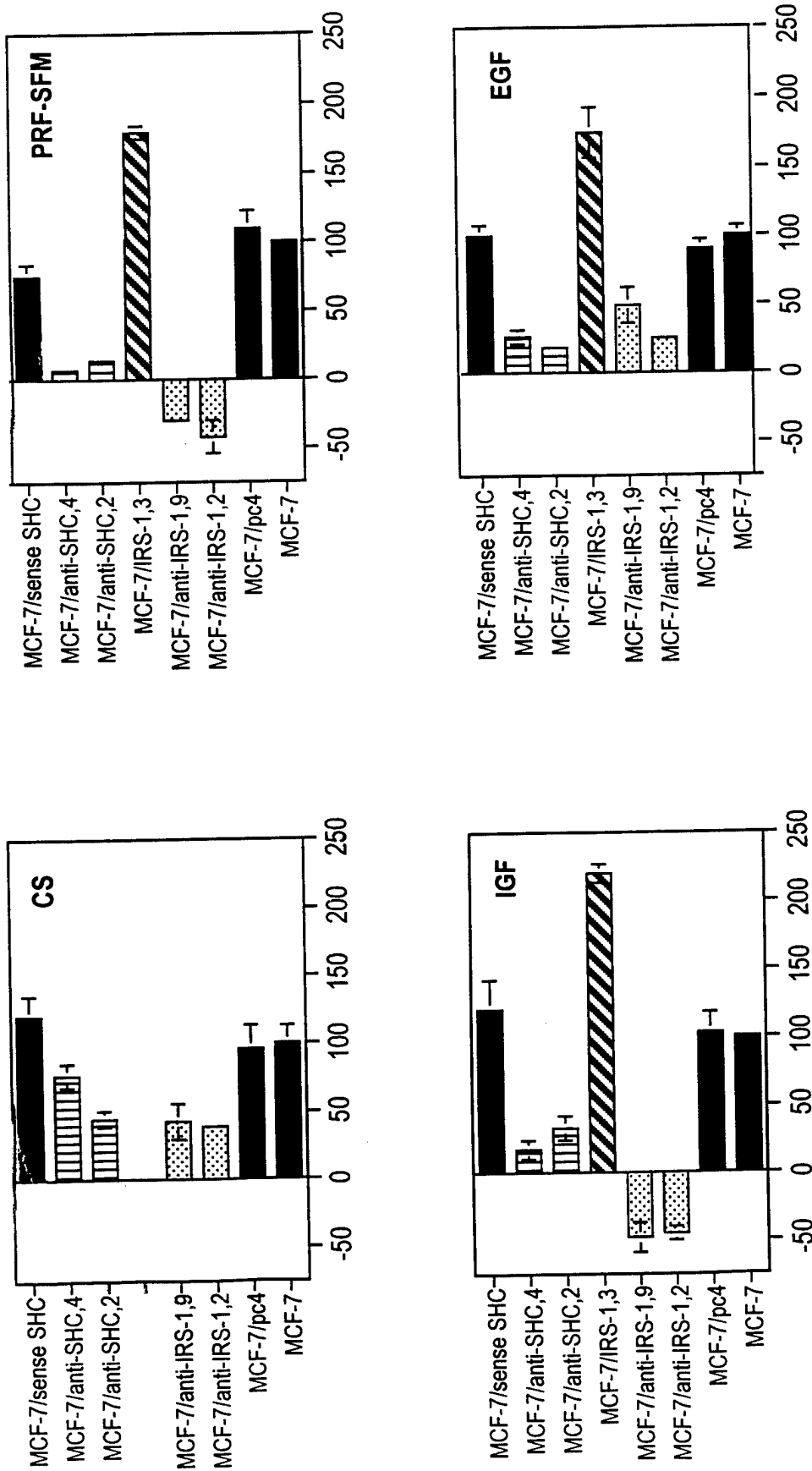


FIG. 2

Relative Growth Increase (%)



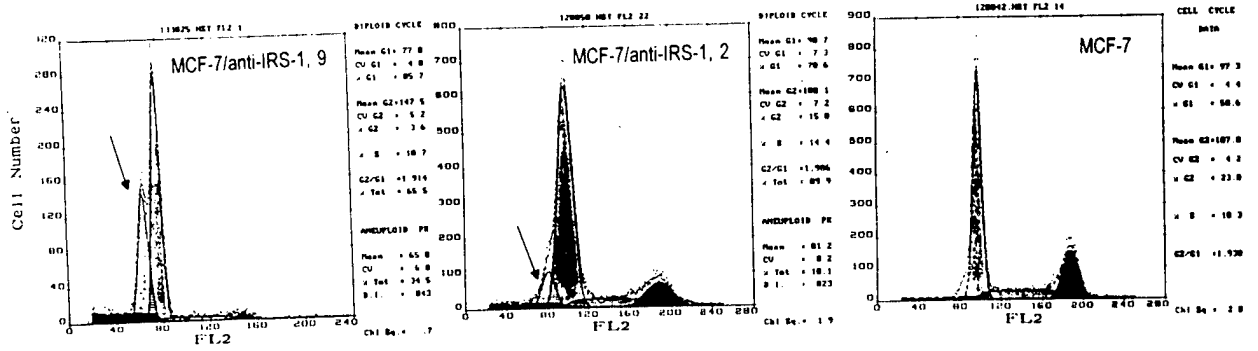


FIG. 3

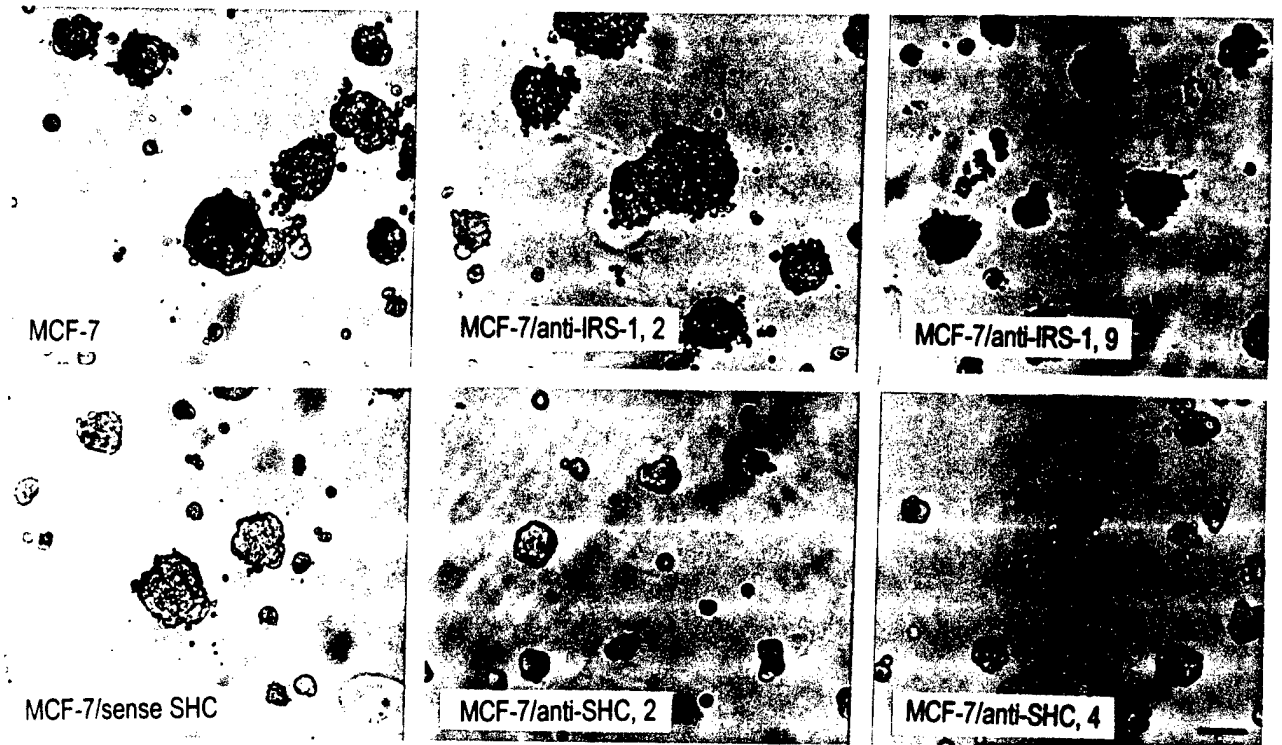


FIG. 4